Stress Testing Credit Portfolios under Geopolitical Risk*

Guillaume Flament†, Christophe Hurlin‡, Quentin Lajaunie§, Yoann Pull¶

January 15, 2026

Abstract

We study how exogenous geopolitical risk (GPR) shocks transmit to U.S. bank credit risk. Relative to standard supervisory stress-testing practices—which rely on published macro scenarios combined with ad hoc, institution-specific PD satellites—we propose a coherent *VAR–Merton* pipeline that links GPR, macro and financial conditions to portfolio default probabilities (PD) through a latent systematic factor Z. A recursively identified VAR estimated on a long macro–financial sample (1986:Q1–2024:Q4) delivers internally consistent impulse paths; a Merton satellite, estimated on the available default-rate window (2015:Q3–2024:Q4), maps these paths into PD dynamics using a closed-form expression for generalized impulse responses. In our U.S. application, a one-standard-deviation GPR shock raises volatility on impact, depresses real equity prices by about 2% at short horizons, lowers the systematic factor by roughly 0.15 standard deviations around 5–6 quarters, and increases portfolio PD by about 0.11 percentage points (about 14% of a 0.79% baseline) around 6–7 quarters before mean reversion. The framework complements supervisory practice by preserving comparability while adding dynamic consistency and an analytic macro-to-PD bridge.

Keywords: Geopolitical risk; macro–finance; VAR; Merton model; default probabilities; stress testing.

JEL codes: C32; E32; E44; G01; G21.

*We sincerely thank David Alcaud and Cyril Regnier for their valuable insights and feedback. This research benefits from the support of the Square Research Center.

†Square Research Center, Rue des poissonniers, 92220, Neuilly-sur-Seine

‡University of Orléans (LEO) and Institut Universitaire de France (IUF), Rue de Blois, 45067 Orléans, France. Corresponding author: christophe.hurlin@univ-orleans.fr

§Square Research Center, Rue des poissonniers, 92220, Neuilly-sur-Seine & University of Orléans (LEO), Rue de Blois, 45067 Orléans, France.

¶Square Research Center, Rue des poissonniers, 92220, Neuilly-sur-Seine & University of Orléans (LEO), Rue de Blois, 45067 Orléans, France.

1 Introduction

Geopolitical tensions have become a first-order driver of macro-financial conditions. Spikes in uncertainty, abrupt asset repricing and real-side slowdowns challenge banks' risk management and supervisory stress testing. While there is substantial evidence on the macro and asset-pricing effects of geopolitical shocks, less is known about their transmission to bank default risk within a single, transparent and dynamically coherent pipeline.

The Financial Stability Review of May 2025 published by the European Central Bank ECB (2025) identifies geopolitical tensions as a key source of financial vulnerability. The report emphasizes the surge in market volatility triggered by the abrupt announcement of new U.S. tariffs in April 2025, alongside the persistent conflict in Ukraine—both contributing to elevated uncertainty and financial instability. This heightened concern is echoed in recent global risk perception surveys. The Global Risk Report 2025 World Economic Forum (2025) ranks geopolitical risk as the most likely to materialize in the coming year, with one-third of respondents anticipating its realisation. Similarly, AXA's Future Risks Report 2024 AXA (2024) places geopolitical risk in second position—just behind climate change—marking an upward shift compared to the 2023 edition, according to expert assessments.

The European Central Bank (ECB) has recently placed geopolitical risk at the heart of its supervisory priorities. According to the ECB Banking Supervision framework, "geopolitical risk is not a new risk. It is a cross-cutting risk driver that can have an impact on banks' traditional risk categories," including credit, market, operational and funding risks.[1] The ECB notes that such risks can materialize through direct exposures to countries or counterparties affected by conflict, or indirectly via macro-financial channels such as trade fragmentation, energy market disruptions, cyber incidents, or supply chain shocks. These interconnections make geopolitical uncertainty a structural vulnerability for the European banking sector rather than a transient shock.

In her September 2025 blog post, ECB Supervisory Board Chair Claudia Buch underscored the evolving role of stress testing as a supervisory instrument in this environment of heightened uncertainty.[2] She emphasized that traditional top-down stress tests, while essential for assessing system-wide resilience, cannot fully capture the range of shocks that may emerge in a world marked by geopolitical fragmentation and complex interdependencies. She therefore called for complementing these exercises with forward-looking, exploratory and bottom-up tools, in

[1] ECB Banking Supervision (2025), Geopolitical risk: supervisory priorities and expectations, Priorities & risks.

[2] Claudia Buch (2025), Looking beyond the immediate horizon: what's next for stress testing?, ECB Banking Supervision Blog, 5 September 2025.

which banks and supervisors jointly explore how non-linear shocks—such as those triggered by geopolitical crises—propagate through balance sheets and business models. Buch described stress testing as a learning device rather than a static compliance exercise: one that should help both banks and supervisors understand vulnerabilities beyond the immediate horizon by quantifying the resilience of institutions under novel risk configurations. This view explicitly links supervisory stress testing to risk discovery and highlights the need for methodological transparency and dynamic coherence.

This strategic reorientation is being operationalized through forthcoming exercises. As reported by the ECB, the 2026 ECB stress test will, for the first time, focus explicitly on geopolitical risk. Banks will be required to construct institution-specific geopolitical scenarios, identifying channels through which tensions—ranging from armed conflict to trade sanctions, cyberattacks or energy supply shocks—could impair their solvency and liquidity positions. In parallel, the ECB will run a reverse stress test for geopolitical risks as part of the ICAAP 2026, asking banks to determine the magnitude and nature of shocks that would render their capital positions non-viable. Together, these initiatives mark a shift from pre-defined, top-down stress designs toward more endogenous, scenario-agnostic frameworks that demand analytical coherence and transparency in tracing macro-financial transmission mechanisms.

From a technical standpoint, our paper builds a bridge between macro-financial modelling and credit portfolio risk measurement by combining a Gaussian Vector Autoregression (VAR) and a Merton-type credit satellite into a single analytical pipeline. This VAR–Merton framework addresses three major limitations of current stress-testing methodologies. First, traditional supervisory exercises rely on exogenous macro scenarios, which ensures comparability but lacks dynamic consistency: macro paths are externally imposed rather than generated endogenously by a model that links GDP, unemployment, markets and spreads through coherent joint dynamics. Our framework endogenizes scenario generation through a Bayesian VAR, ensuring that macro-financial variables evolve jointly according to historical propagation patterns. Second, we close the transmission gap between macroeconomic shocks and credit outcomes by replacing ad hoc stress multipliers with a structural credit-risk mapping grounded in the Merton–Vasicek framework. The latent systematic factor inferred from observed default rates is regressed on macro-financial variables selected from the VAR, producing a theoretically consistent and auditable macro-to-credit bridge. Third, we introduce an analytic mapping from macro shocks to portfolio default probabilities: instead of relying on Monte Carlo simulation, we derive a closed-form generalized impulse response function that accounts for the nonlinearity of the Merton transformation. This yields a fully transparent and computationally efficient propagation

of uncertainty from shocks to credit outcomes.

Together, these elements make the VAR–Merton pipeline replicable, auditable and policy-compatible. It complements rather than replaces the EBA-style stress-testing architecture: published scenarios can still be used as inputs, but our framework adds dynamic coherence and produces PD responses consistent with the underlying macro-financial dynamics. The approach is flexible enough to accommodate alternative identification schemes or non-geopolitical shocks, making it directly applicable to ICAAP and supervisory exercises, including the forthcoming ECB 2026 geopolitical and reverse stress tests.

In our U.S. application, a one-standard-deviation GPR shock raises the VIX on impact and lowers real equity prices by about 2% at short horizons; activity weakens over subsequent quarters. The implied path for the systematic factor Z troughs near -0.15 standard deviations at horizons 5–6 quarters and, through the Merton mapping, raises portfolio PD by about 0.11 percentage points (roughly 14% of a 0.80% baseline) at horizons 6–7 before mean reversion. These magnitudes and timings align with supervisory planning windows and are readily translatable into capital and provisioning exercises.

The remainder of the paper details the framework, presents the U.S. evidence, and discusses robustness and implementation issues for banks and supervisors.

2 Literature review

2.1 Measuring geopolitical risk

Geopolitical risk has long been a subject of economic research, with early contributions examining the macroeconomic consequences of both terrorism (e.g., Eckstein and Tsiddon, 2004; Blomberg et al., 2004) and war (e.g., Glick and Taylor, 2010; Blattman and Miguel, 2010). Abadie and Gardeazabal (2003), for instance, examine the Basque terrorist conflict using a synthetic control method and show that the onset of violence in the late 1960s reduced per capita GDP by roughly 10% relative to a comparable counterfactual region. The economic effects of war are similarly well documented. Using a comprehensive dataset spanning 1870–1997, Glick and Taylor (2010) demonstrate that wars produce severe and persistent disruptions in bilateral trade, leading to long-term output losses. Blattman and Miguel (2010) review the empirical literature on civil wars, showing that conflict depresses economic development through the destruction of physical and human capital, the weakening of institutions, and the deterrence of private investment. Complementing these macroeconomic perspectives, a parallel literature examines the influence of war-related events on financial markets (e.g., Rigobon and Sack, 2005; Choudhry, 2010).

While early contributions focused on specific manifestations of geopolitical risk, more recent work has sought to construct systematic, time-varying indicators that capture geopolitical tensions across countries. A key development in this respect is the geopolitical risk (GPR) index proposed by Caldara and Iacoviello (2022), constructed through automated text analysis of major newspapers. The index provides a consistent and replicable measure of geopolitical tensions, defined as *"threat, realisation, and escalation of adverse events associated with wars, terrorism, and any tensions among states and political actors that affect the peaceful course of international relations"*. Unlike indicators designed for specific types of geopolitical episodes, the GPR index offers an integrated measure of both the anticipation and the realisation of shocks. This feature is particularly valuable for bank stress-testing frameworks, where geopolitical risk is multidimensional, heterogeneous across exposures, and characterised by uncertainty about whether threats will materialise.

Formally, the GPR index is constructed from the frequency of newspaper articles published in the United States, the United Kingdom, and Canada that report on geopolitical events. These sources are selected to capture news with global relevance and broad international repercussions. Using a dictionary of keywords related to war, peace, military activity, nuclear issues, terrorism, and associated threat or action terms ("risk," "crisis," "threat," "attack," "invasion," "bombing"), the authors build two sub-indices: the Geopolitical Threats Index (GPT), capturing tensions and military buildups, and the Geopolitical Acts Index (GPA), capturing the realisation and escalation of adverse events. The aggregate GPR index is available at a daily frequency from 1985 onward, for 44 countries. Figure 1 illustrates its evolution for the United States.

Alternative measures of geopolitical risk exist, including the GDELT database (Shawon et al., 2024; Wei et al., 2024), which relies on machine-coded global news events, and event-based approaches such as Engle and Campos-Martins (2023). Proprietary indicators developed by investment funds, such as Amundi's Geopolitical Sentiment Tracker (GST) or BlackRock's Geopolitical Risk Indicator (BGRI), also provide useful insights. However, these alternatives typically depend on narrower or less transparent data sources, rely on more complex classification methods, or offer weaker interpretability for scenario design.

By contrast, the GPR index delivers a systematic and economically interpretable measure of geopolitical risk. Its explicit distinction between the *threat* and the *realisation* of events is especially valuable, as anticipated conflict, sanctions, or political shocks can affect financial markets even without materialisation. In addition, because the GPR index is constructed independently of macroeconomic and financial variables, it captures genuinely exogenous geopolitical shocks rather than endogenous economic responses. These properties make the index particularly

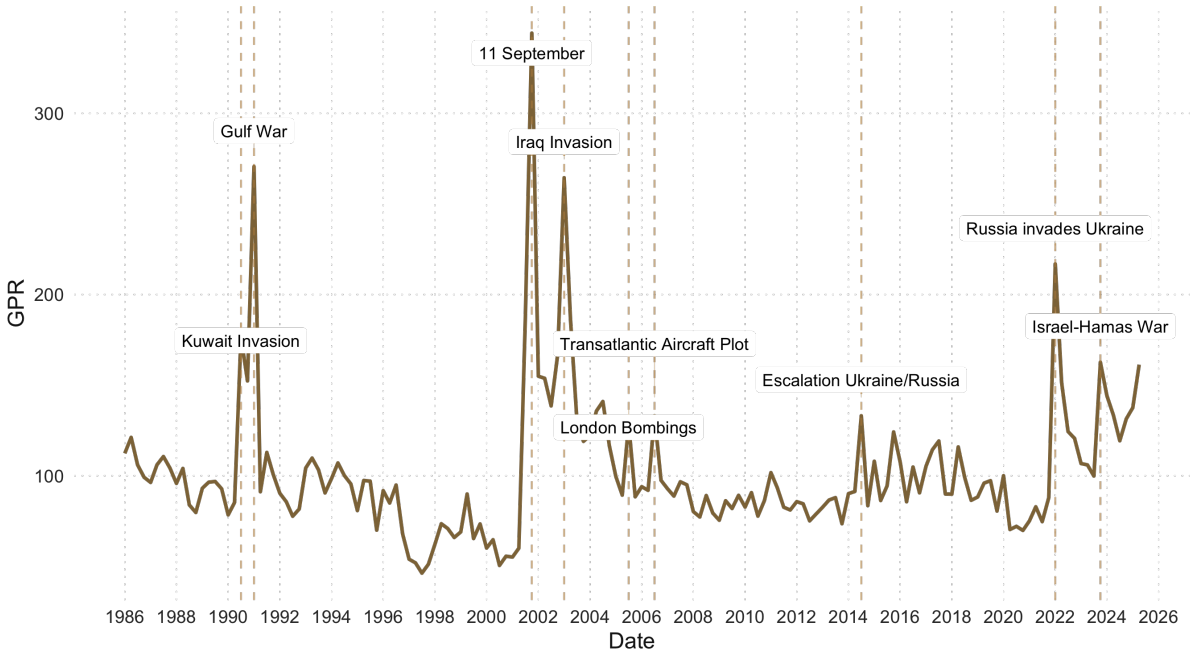

Figure 1: Geopolitical risk index. *Notes: Quarterly averages of the geopolitical risk (GPR) index, covering the period from 1986:Q1 to 2024:Q4.*

well suited for credit portfolio stress testing, where geopolitical uncertainty may arise from heterogeneous sources across counterparties, sectors, and regions.

The GPR index has therefore become the benchmark for analysing geopolitical tensions and their economic consequences. As of October 2025, the paper by Caldara and Iacoviello (2022) had accumulated more than 4,100 citations on Google Scholar. A growing empirical literature documents its effects on financial markets, showing that higher geopolitical risk increases volatility and reduces returns (Bouras et al., 2019; Umar et al., 2022), and on macroeconomic outcomes, including investment, consumption, and industrial production. Pinchetti (2025), for example, identifies two distinct channels through which geopolitical shocks operate: energy-related shocks that are both inflationary and recessionary, and macro shocks that are deflationary and contractionary.

More recently, attention has shifted toward the banking sector, giving rise to a growing literature on the implications of geopolitical risk for financial stability. Behn et al. (2025) show that only exceptionally high levels of geopolitical risk significantly erode banks' capital ratios. Phan et al. (2022) document a negative relationship between geopolitical risk and bank stability, underscoring the mitigating role of capital buffers and bank size. Nguyen and Thuy (2023) find that heightened geopolitical tensions raise borrowing costs and tighten nonprice loan terms in the United States, while Zhu et al. (2025) show that global geopolitical risk amplifies financial stress connectedness across Chinese sectors. Wang et al. (2025) further provide cross-country evidence

that geopolitical risk increases systemic fragility by raising bank risk and contributing to asset price bubbles. Reflecting the policy relevance of this literature, institutions such as the ECB and the IMF now explicitly incorporate geopolitical risk into their financial stability assessments (Dieckelmann et al., 2024; IMF, 2023). However, despite these advances, no academic study to date has examined the direct link between geopolitical risk and credit risk through loan portfolio stress testing. Our analysis fills this gap.

2.2 Linking geopolitical risk to credit risk through stress testing

How can geopolitical risk be translated into credit risk, and more specifically into the default dynamics of banks' loan portfolios? The most natural analytical framework to operationalize this link is stress testing. As underlined by Claudia Buch, Chair of the Supervisory Board of the European Central Bank (ECB), "*stress tests are a key tool to understand how banks would respond under adverse conditions and to ensure that they remain resilient in a rapidly changing risk environment.*"[3] In a context where geopolitical shocks are increasingly shaping the macro-financial outlook, stress testing offers a disciplined way to quantify how rising geopolitical tensions propagate through economic activity, and ultimately, bank credit losses.

Modern stress-testing frameworks are structured scenario analyses of severe-yet-plausible conditions designed to assess both banks' and the system's resilience (Quagliariello, 2009). They consist of four integrated blocks: (i) scenario design; (ii) satellite models that translate exogenous macro shocks into the endogenous risk parameters driving credit risk such as point-in-time probabilities of default (PDs), and loss-given-defaults (LGDs); (iii) balance-sheet mechanics capturing risk-weighted asset (RWA) dynamics; and (iv) feedback effects reflecting second-round and system-wide amplifications (Henry and Kok, 2013; Borio et al., 2014). Updated supervisory guidance has codified these elements across jurisdictions (Budnik et al., 2024; Adrian et al., 2020; European Banking Authority, 2025; Board of Governors of the Federal Reserve System, 2025; Bank of England, 2024).

Within this architecture, the *credit satellite* represents the transmission channel between the macro-financial scenario and default risk parameters. It links GDP growth, unemployment, or financial spreads to PIT PDs and LGDs, which feed the balance-sheet engine and determine capital depletion. Two structural traditions dominate this block: the Merton–Vasicek ASRF model, which defines default as a latent threshold event under a Gaussian factor and delivers the closed-form link between through-the-cycle and point-in-time default probabilities underpinning Basel II/III and IFRS 9 (Merton, 1974; Vasicek, 2002); and J.P. Morgan's *CreditMetrics*, which

[3]This definition comes from the ECB Banking Supervision Blog, *"Stress tests in uncertain times: assessing banks' resilience to external shocks,"* 5 September 2025.

extends this logic to rating migrations through ordered-probit transitions driven by systematic factors (Belkin et al., 1998; Gouriéroux and Tiomo, 2007).

Geopolitical shocks challenge this framework by introducing exogenous, non-economic triggers that can shift the entire risk landscape. Episodes of rising geopolitical tension, captured by sudden increases in the GPR index, can tighten financial conditions, depress investment, and increase sovereign and corporate risk premia. Incorporating such shocks into stress-testing design allows one to move beyond traditional macro scenarios and assess how geopolitical uncertainty translates into higher PDs and LGDs. In practice, the GPR index can serve as a *scenario generator*, with identified spikes mapped into adverse macro-financial trajectories using historical elasticities or econometric models. These scenarios can then be propagated through the credit satellite to quantify portfolio-level credit losses.

Reverse stress-testing complements this approach by inverting the logic: starting from a failure outcome, such as a breach of the Pillar 2 Guidance capital threshold, and asking which level of geopolitical escalation, proxied by the GPR index, could plausibly produce it. This approach identifies critical thresholds at which geopolitical tensions would trigger widespread defaults or capital depletion, highlighting non-linearities and feedback loops that traditional scenario analyses may miss. As Claudia Buch notes, reverse stress-testing is especially relevant in times of "*greater uncertainty and more complex risk interactions*," such as those induced by geopolitical fragmentation.

Our contribution builds on this conceptual bridge between geopolitical and credit risk. First, we endogenize scenario generation by embedding identified BVAR shocks in the GPR index sequence to ensure dynamic coherence between geopolitical and macro-financial variables. Second, we derive an analytical macro→PD bridge delivering closed-form generalized impulse response functions (GIRFs) for PDs, removing the need for Monte Carlo simulation. Third, we propagate uncertainty from the GPR shock to the full PD distribution, providing predictive intervals for defaults and capital adequacy. The resulting framework integrates geopolitical risk into supervisory stress testing in a transparent, auditable, and dynamically consistent way.

3 General framework

Geopolitical risks are more uncertain and unpredictable than traditional risks. They can have immediate and profound consequences that are often difficult to anticipate. These risks are exogenous to the financial system and are transmitted mainly through three channels: (i) financial markets, (ii) the real economy, (iii) safety and security (Buch, 2024). They thus generate macrofinancial effects that have repercussions on banks and their traditional risks.

Our methodological framework traces the transmission of a geopolitical risk shock through the macroeconomy and ultimately to corporate probabilities of default (PD). The analysis proceeds in two steps, combining a macroeconomic model of shock propagation with a credit risk satellite model. First, we estimate a Gaussian VAR on an n-dimensional vector Y_t that includes the geopolitical risk index together with a set of macroeconomic variables, in order to capture their dynamic interactions while treating the geopolitical risk index as exogenous. Using time series of observed portfolio default rates, we then compute the systematic factor Z_t from Merton's model, which summarizes economic conditions based on historical defaults. This factor is subsequently regressed on the same set, or on a subset, of the variables included in the VAR, denoted $Y_t^{(s)}$, to establish its relationship with real economic activity. In line with the stress testing literature, this second model is referred to as the *satellite model*.

Second, we trace how shocks to the GPR index are transmitted to default risk through the macroeconomic block. We compute generalized impulse response functions (GIRFs, in the sense of Koop et al., 1996) from the estimated VAR, treating a one–standard–deviation innovation in the GPR index as the shock of interest. The implied trajectories of the macroeconomic variables over the forecast horizon are then fed into the satellite model estimated in the first step. The nonlinear Merton model mapping from macroeconomic conditions to default probabilities implies that conventional linear IRFs cannot be directly translated into responses of default risk. By contrast, our GIRF-based procedure delivers impulse responses of PDs that remain valid under this nonlinearity and, in the linear case, are consistent with the ordering–invariant generalized IRFs of Pesaran and Shin (1998).

Figure 2 summarizes the approach, and the following subsections provide additional details.

3.1 The VAR–Merton framework

In the first step, we combine two components. The first is a Gaussian VAR that captures the joint dynamics between the geopolitical risk index and key macroeconomic aggregates. The second is a Merton–type satellite model that translates macroeconomic conditions into portfolio default probabilities. These two components are estimated independently, and their connection is established in the subsequent section

3.1.1 Macroeconomic dynamics

Let G_t denote the geopolitical risk index and let $\mathbf{X}_t = (X_{1,t}, \ldots, X_{n-1,t})^\top \in \mathbb{R}^{n-1}$ collect the remaining macroeconomic variables. We stack them as

$$Y_t = (G_t,\ \mathbf{X}_t^\top)^\top \in \mathbb{R}^n.$$

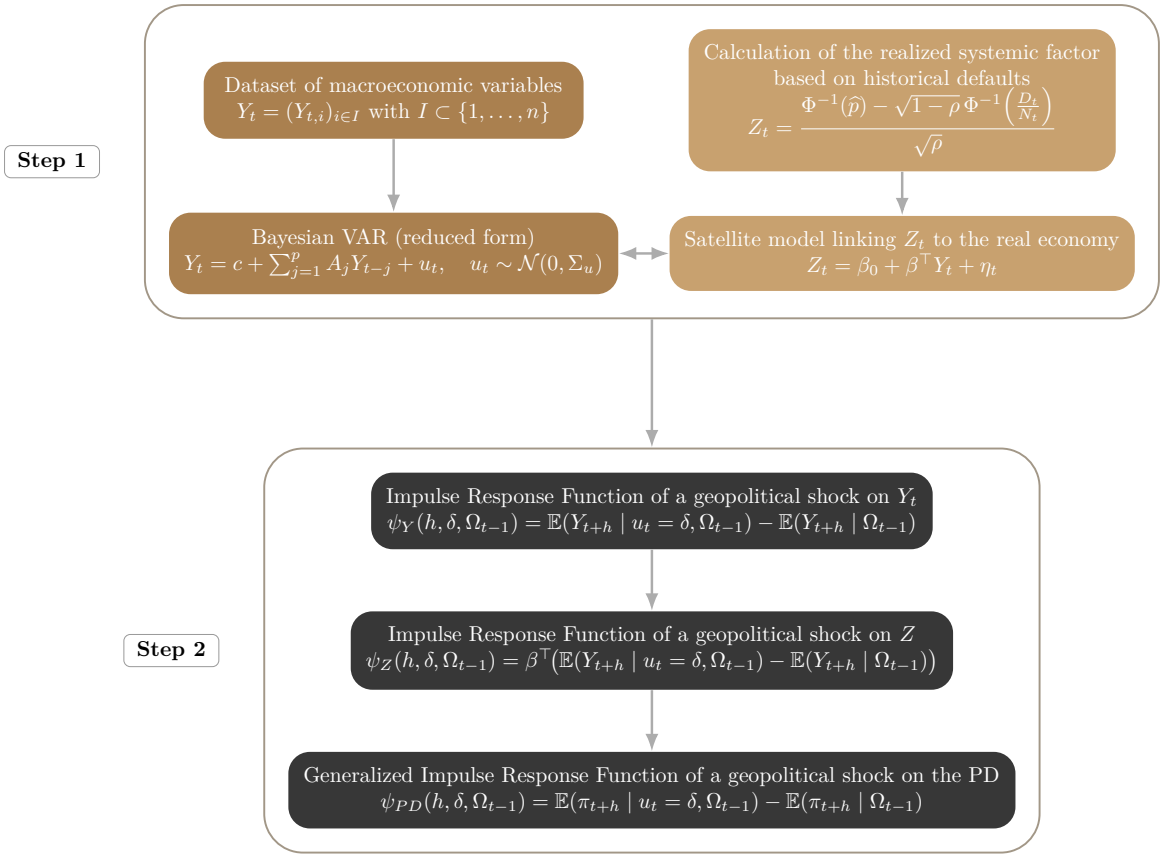

Figure 2: A two-step approach
Notes: Summary of the two-step approach for analyzing the impact of a geopolitical shock on a loan portfolio.

The VAR(p) model is given by

$$Y_t = c + \sum_{i=1}^{p} A_i Y_{t-i} + u_t, \qquad u_t \overset{\text{i.i.d.}}{\sim} \mathcal{N}(\mathbf{0}_n, \Sigma_u), \quad t \in \mathbb{Z}, \tag{3.1}$$

where $c \in \mathbb{R}^n$, $A_i \in \mathbb{R}^{n \times n}$, and $\Sigma_u \succ 0$. Following Caldara and Iacoviello (2022), we estimate the model using Bayesian methods by imposing a Normal–Inverse–Wishart (NIW) prior on $(A_1, \ldots, A_p, c, \Sigma_u)$; that is, an inverse–Wishart prior on Σ_u and a conjugate normal prior on the coefficient matrices.

Consistent with Caldara and Iacoviello (2022), we impose no prior restrictions on the coefficients of the VAR equation for the GPR index, allowing all lagged macroeconomic variables to affect it.

3.1.2 Default risk dynamics via a Merton satellite model

We translate macroeconomic conditions into default risk through a one-factor structure grounded in the Merton framework (Merton (1974); Vasicek (2002)). In this standard specification, the point-in-time probability of default for firm i conditional on the latent systematic factor Z_t is

$$\pi_i(Z_t) = \Phi\left(\frac{\Phi^{-1}(p_i) - \sqrt{\rho}\, Z_t}{\sqrt{1-\rho}}\right), \tag{3.2}$$

where $p_i \in (0,1)$ denotes the unconditional (long-run average) PD, $\rho \in [0,1[$ the asset correlation, and $\Phi(\cdot)$ the standard normal cumulative distribution function (CDF).

The calibration of the parameters and the reconstruction of the time series of the systemic factor Z_t are based on the observed portfolio default rates $\{d_1, \ldots, d_T\}$ over an estimation sample of T periods. The long–run portfolio PD p_i is estimated as the empirical average of the observed default rates over this window:

$$\widehat{p}_i = \frac{1}{T}\sum_{t=1}^{T} d_t, \tag{3.3}$$

where each $d_t \in (0,1)$ denotes the default rate of the portfolio at time t. Interpreting the observed default rate d_t as a noisy sample of the conditional default probability $\pi_i(Z_t)$, the latent factor implied by equation (3.2) for a given value of the asset correlation parameter ρ is obtained as

$$Z_t(\rho, \widehat{p}_i) = \frac{\Phi^{-1}(\widehat{p}_i) - \sqrt{1-\rho}\,\Phi^{-1}(d_t)}{\sqrt{\rho}}. \tag{3.4}$$

To ensure comparability with the standard Merton and Vasicek framework, we calibrate the asset correlation parameter by selecting the value $\hat{\rho} \in [0,1[$ that satisfies $\mathrm{Var}_t[Z_t(\widehat{\rho}, \widehat{p}_i)] = 1$, so that the reconstructed latent factor has unit unconditional variance. We then define $Z_t := Z_t(\hat{\rho}, \widehat{p}_i)$ which serves as our estimate of the systematic factor.

The final component of our framework is the satellite model that relates the estimated systematic factor Z_t to macroeconomic conditions. If the Merton structure holds, the systematic component of credit risk should co-move with observable macroeconomic variables. Let $Y_t^{(s)} \subseteq \{Y_t, \ldots, Y_{t-q}\}$ denote the subset of variables and lags selected for the satellite equation. We specify the reduced-form relationship as

$$Z_t = \beta_0 + \beta^\top Y_t^{(s)} + \eta_t, \qquad \eta_t \sim \mathcal{N}(0, \sigma_\eta^2), \quad \mathbb{E}[\eta_t \mid Y_t^{(s)}] = 0, \tag{3.5}$$

and estimate (β_0, β) by OLS using the reconstructed factor series $\{Z_t\}_{t=1}^T$. This satellite block provides the empirical bridge through which macroeconomic conditions, captured in the VAR, are mapped into systematic credit risk. The selection procedure of the variables and lags included in $Y_t^{(s)}$ will be detailed in Section 3.2.2.

3.2 Shock transmission from GPR to default risk

In this section, we investigate how shocks to the GPR index are transmitted to default risk through the macroeconomic block of the model. To this end, we use generalized impulse response functions (GIRFs) to study the dynamic effects of GPR shocks. We compute GIRFs to a one standard deviation innovation in the GPR index and feed the implied trajectories of macroeconomic variables over the forecast horizon into our framework. Because default

probabilities are obtained from these macroeconomic paths through the bounded and nonlinear mapping in equation 3.2, conventional linear IRFs cannot be directly translated into responses of default risk. GIRFs, in the sense of Koop et al. (1996), remain valid under nonlinearity and are consistent with the ordering-invariant generalized IRFs of Pesaran and Shin (1998) in the linear case.

3.2.1 Generalized impulse responses of macroeconomic variables

To study the transmission of GPR shocks to the macroeconomy, we compute generalized impulse response functions (GIRFs) from the VAR in equation (3.1). We interpret an innovation in the GPR index as the shock of interest and trace its dynamic effects on the remaining variables. A practical advantage of GIRFs is that they do not require a recursive identification scheme, so we do not need to commit to a particular ordering of the shocks in Y_t.

Before proceeding, we introduce some notation. We keep the notation from the previous section and let Ω_{t-1} denote the information set at time $t-1$, that is, the set of all possible histories of the process up to $t-1$. A particular realization of this history is denoted by $\omega_{t-1} \in \Omega_{t-1}$. Let $g \in \{1, \ldots, n\}$ be the index of the GPR variable in Y_t, and let $e_g \in \mathbb{R}^n$ denote the g-th canonical unit vector (with a 1 in position g and zeros elsewhere). The reduced–form innovation to the GPR index is then

$$u_{gt} \;=\; e_g' u_t.$$

Definition 1 (**Generalized impulse response function**). *For a horizon $h \geq 0$, a history $\omega_{t-1} \in \Omega_{t-1}$, and a reduced–form shock vector $\delta \in \mathbb{R}^n$ applied to u_t, the generalized impulse response function (GIRF) of the vector Y_t is defined as*

$$\psi_Y(h, \delta, \omega_{t-1}) := \mathbb{E}[Y_{t+h} \mid u_t = \delta,\ \Omega_{t-1} = \omega_{t-1}] - \mathbb{E}[Y_{t+h} \mid \Omega_{t-1} = \omega_{t-1}]. \tag{3.6}$$

As emphasized by Pesaran and Shin (1998), instead of shocking all components of u_t, we may focus on shocks to a single component, here the GPR innovation.

Definition 2 (**GIRF to a GPR shock**). *Let g denote the index of the GPR variable in Y_t and let $u_{gt} = e_g' u_t$ be its reduced–form innovation. For a horizon $h \geq 0$, a history $\omega_{t-1} \in \Omega_{t-1}$, and a scalar shock size $\delta_g \in \mathbb{R}$ applied to u_{gt}, the generalized impulse response function of Y_t to a GPR shock is defined as*

$$\psi_Y^g(h, \delta_g, \omega_{t-1}) := \mathbb{E}[Y_{t+h} \mid u_{gt} = \delta_g,\ \omega_{t-1}] - \mathbb{E}[Y_{t+h} \mid \omega_{t-1}]. \tag{3.7}$$

Let $\{\Psi_h\}_{h \geq 0}$ denote the moving–average coefficients of the VAR, so that

$$Y_t = \mu + \sum_{h=0}^{\infty} \Psi_h u_{t-h}, \qquad \Psi_0 = I_n, \tag{3.8}$$

and let $\Sigma_u = \mathrm{Var}(u_t)$ with (g,g)-element σ_{gg}. In a linear Gaussian VAR, the GIRF does not depend on the particular history ω_{t-1}, and Pesaran and Shin (1998) show that, for a one–standard–deviation shock $\delta_g = \sigma_{gg}^{1/2}$ to the GPR innovation, the (scaled) generalized impulse response function can be written as

$$\psi_Y^g(h) \;=\; \sigma_{gg}^{-1/2}\Psi_h\Sigma_u e_g. \tag{3.9}$$

An important property in the linear VAR case is that the GIRF to a shock in the g-th variable coincides with the orthogonalized impulse response function (OIRF) obtained from a Cholesky decomposition in which this variable is ordered first. This follows from the ordering–invariance property of generalized impulse responses together with Proposition 3.1 in Pesaran and Shin (1998). It means that, for our purposes, the GIRF to a GPR innovation coincide to the OIRF one would obtain from a recursively identified VAR in which the GPR index is placed first in the Cholesky ordering. The relative ordering of the remaining variables is immaterial for this equivalence, as it does not affect the responses to a shock in the GPR index.

3.2.2 Propagating GIRFs through lag-selection operators

Because the satellite equation uses subsets and lags of the VAR variables it is convenient to introduce a linear lag-selection operator that compacts notation and preserves linearity.

Definition 3 (**Linear operator representation with lags**). *Let L denote the lag operator, with $L^\ell x_t := x_{t-\ell}$ for $\ell \in \mathbb{N}_0$. For $Y_t \in \mathbb{R}^n$ and a maximum lag $L_{\max} \in \mathbb{N}_0$, define the polynomial selection operator*

$$S^{(s)}(L) := \sum_{\ell=0}^{L_{\max}} S_\ell^{(s)}\, L^\ell, \qquad S_\ell^{(s)} \in \{0,1\}^{m\times n}. \tag{3.10}$$

The selected vector is then the linear transform

$$Y_t^{(s)} = S^{(s)}(L)\, Y_t = \sum_{\ell=0}^{L_{\max}} S_\ell^{(s)}\, Y_{t-\ell} \in \mathbb{R}^m. \tag{3.11}$$

Each row of the block matrices $\{S_\ell^{(s)}\}_{\ell=0}^{L_{\max}}$ contains exactly one entry equal to 1 across all lags (and zeros elsewhere), thereby selecting exactly one component $(Y_{t-\ell})_j$ per row. Equivalently, defining the stacked state vector $\widetilde{Y}_t = \big((Y_t)^\top, \ldots, (Y_{t-L_{\max}})^\top\big)^\top$, we have

$$Y_t^{(s)} = \underbrace{\big[\, S_0^{(s)} \;\; S_1^{(s)} \;\; \cdots \;\; S_{L_{\max}}^{(s)} \,\big]}_{=:\, S^{(s)}} \widetilde{Y}_t. \tag{3.12}$$

Notice that the g-th column of each selection matrix $S_\ell^{(s)}$ is a zero vector, because the GPR index is therefore never included directly in the satellite regression.

Consider a simple example. Let $Y_t = (\text{GPR}_t,\ \text{GDP growth}_t,\ \text{unemployment}_t)^\top$, where the GPR index is ordered first. Suppose we want to construct a satellite equation that relates the systematic factor Z_t to a vector of macroeconomic indicators consisting of the current value of GDP growth, its second lag, and the first lag of unemployment. To obtain this selection, let $n = 3$, $m = 3$, and choose $L_{\max} = 2$. Define the block selection matrices, with the first column set to zero everywhere to reflect the exclusion of GPR in the satellite model:

$$S_0^{(s)} = \begin{bmatrix} 0 & 1 & 0 \\ 0 & 0 & 0 \\ 0 & 0 & 0 \end{bmatrix}, \qquad S_1^{(s)} = \begin{bmatrix} 0 & 0 & 0 \\ 0 & 0 & 0 \\ 0 & 0 & 1 \end{bmatrix}, \qquad S_2^{(s)} = \begin{bmatrix} 0 & 0 & 0 \\ 0 & 1 & 0 \\ 0 & 0 & 0 \end{bmatrix}. \tag{3.13}$$

Applying this operator to Y_t yields the desired selection:

$$Y_t^{(s)} = S^{(s)}(L)\, Y_t = \left(S_0^{(s)} + S_1^{(s)} L + S_2^{(s)} L^2\right) Y_t = \begin{bmatrix} \text{GDP growth}_t \\ \text{GDP growth}_{t-2} \\ \text{unemployment}_{t-1} \end{bmatrix}. \tag{3.14}$$

By linearity and time invariance, GIRFs propagate through the selection operator as a simple convolution over lags:

Proposition 1 (**GIRFs for the satellite explanatory vector** $Y^{(s)}$)**.** *Let* $Y_t^{(s)} = S^{(s)}(L)\, Y_t$ *be the vector of explanatory variables entering the satellite equation, where* $Y_t \in \mathbb{R}^n$ *denotes the VAR vector and* $S^{(s)}(L)$ *is the lag-selection operator introduced in Definition 3. Then, for any horizon* $h \geq 0$*, history* ω_{t-1}*, and reduced–form shock* $\delta_g \in \mathbb{R}$*, the GIRF for the satellite explanatory vector* $Y^{(s)}$ *is*

$$\psi^g_{Y^{(s)}}(h, \delta_g, \omega_{t-1}) \;=\; S^{(s)}(L)\, \psi^g_Y(h, \delta_g, \omega_{t-1}) \;=\; \sum_{\ell=0}^{L_{\max}} S_\ell^{(s)}\, \psi^g_Y(h-\ell, \delta_g, \omega_{t-1}), \tag{3.15}$$

with the convention $\psi^g_Y(h', \cdot, \cdot) \equiv 0$ *for* $h' < 0$*.*

The proof of Proposition 1 is reported in Appendix A.1. The GIRF for the systematic factor Z follows directly from the satellite regression by applying the same linear operator:

Proposition 2 (**GIRF for the systematic factor**)**.** *Let the systematic factor* Z *defined by* $Z_t = \beta_0 + \beta^\top Y_t^{(s)} + \eta_t$*, with* $\mathbb{E}[\eta_t \mid \cdot] = 0$*, and where* $Y_t^{(s)} = S^{(s)}(L) Y_t$*,* $Y_t \in \mathbb{R}^n$ *denotes the VAR vector, and* $S^{(s)}(L)$ *is the lag-selection operator introduced in Definition 3. Then, for any* $h \geq 0$ *and* $\delta_g \in \mathbb{R}$*, the GIRF for the systematic factor* Z *is defined as*

$$\psi^g_Z(h, \delta_g, \omega_{t-1}) = \beta^\top S^{(s)}(L)\, \psi^g_Y(h, \delta_g, \omega_{t-1}) = \sum_{\ell=0}^{L_{\max}} \beta^\top S_\ell^{(s)}\, \psi^g_Y(h-\ell, \delta_g, \omega_{t-1}), \tag{3.16}$$

with the convention $\psi^g_Y(h', \cdot, \cdot) \equiv 0$ *for all* $h' < 0$*.*

Proof. Write $Y_{t+h}^{(s)} = \sum_\ell S_\ell^{(s)} Y_{t+h-\ell}$ and take conditional expectations; future shocks have zero mean. Subtract the two conditional means term-by-term. □

3.2.3 Closed-form generalized impulse responses for portfolio default probabilities

The final stage of the geopolitical stress-testing procedure is to map the shock-induced trajectory of the systematic factor into portfolio default probabilities in a manner consistent with the nonlinear structure of the Merton model. Given Proposition 2, the GIRF for the systematic factor Z follows directly from the GIRF for the macroeconomic variables in Y. This allows us to propagate geopolitical shock through the VAR and the satellite equation and obtain the entire sequence $\{Z_{t+h}\}_{h\geq 0}$ implied by the disturbance.

To translate this trajectory into portfolio default probabilities, one would ideally feed the paths of Z_{t+h} into the Merton mapping (3.2). However, unlike the linear relations exploited above, the transformation $Z \mapsto \pi_i(Z)$ is nonlinear, so the PD response cannot be obtained through a simple linear transformation of $\psi^g_Z(h, \delta_g, \omega_{t-1})$. Deriving the GIRF for the PIT probability of default $\pi_i(Z)$ therefore requires taking expectations of a nonlinear transformation of a Gaussian random variable. Formally, the GIRF of portfolio default probabilities is defined as

$$\psi^g_{\pi_i(Z)}(h, \delta_g, \omega_{t-1}) := \mathbb{E}\big[\pi_i(Z_{t+h}) \mid u_{gt} = \delta_g,\ \omega_{t-1}\big] - \mathbb{E}\big[\pi_i(Z_{t+h}) \mid \omega_{t-1}\big], \tag{3.17}$$

where h denotes the horizon of the response, ω_{t-1} is the realized history of the system up to time $t-1$, and δ_g is the reduced-form innovation associated with the geopolitical shock.

To obtain a closed-form expression for $\psi^g_{\pi_i(Z)}(h, \delta_g, \omega_{t-1})$, we rely on the following lemma, which characterizes the expectation of the Merton mapping under a Gaussian distribution.

Lemma 1. *Let $W \sim \mathcal{N}(\mu, \sigma^2)$. Then*

$$\mathbb{E}\left[\Phi\left(\frac{\Phi^{-1}(p) - \sqrt{\rho}\, W}{\sqrt{1-\rho}}\right)\right] = \Phi\left(\frac{\Phi^{-1}(p) - \sqrt{\rho}\,\mu}{\sqrt{(1-\rho) + \rho\,\sigma^2}}\right). \tag{3.18}$$

The proof of Lemma 1 is provided in Appendix A.2. We now derive a closed-form expression for the GIRF of portfolio default probabilities. Let the conditional means and variances of the unshocked and shocked normal distributions of the factor Z_{t+h} for $h \geq 0$ be defined as

$$\mu_{t+h} := \mathbb{E}[Z_{t+h} \mid \omega_{t-1}], \qquad \mu^{(\delta_g)}_{t+h} := \mathbb{E}[Z_{t+h} \mid u_{gt} = \delta_g,\, \omega_{t-1}], \tag{3.19}$$

$$s^2_{t+h} := \mathrm{Var}[Z_{t+h} \mid \omega_{t-1}], \qquad (s^{(\delta_g)}_{t+h})^2 := \mathrm{Var}[Z_{t+h} \mid u_{gt} = \delta_g,\, \omega_{t-1}]. \tag{3.20}$$

The GIRF of the default probabilities is given by the following proposition.

Proposition 3 (Closed-form GIRF of the default probabilities). *Under the model specification (3.1)–(3.5), the GIRF of the PIT probability of default $\pi_i(Z)$ at horizon h in response to a shock δ_g to the geopolitical risk index is*

$$\psi^g_{\pi_i(Z)}(h, \delta_g, \omega_{t-1}) = \Phi\left(\frac{\Phi^{-1}(p_i) - \sqrt{\rho}\,\mu^{(\delta_g)}_{t+h}}{\sqrt{(1-\rho) + \rho\,(s^{(\delta_g)}_{t+h})^2}}\right) - \Phi\left(\frac{\Phi^{-1}(p_i) - \sqrt{\rho}\,\mu_{t+h}}{\sqrt{(1-\rho) + \rho\, s^2_{t+h}}}\right). \tag{3.21}$$

The proof of Proposition 3 is reported in Appendix A.3. This closed-form expression provides a direct measure of the effect of a geopolitical shock on portfolio PIT default probabilities at any horizon h. It offers a tractable tool for quantifying how disturbances to the GPR index propagate through macro-financial conditions into portfolio credit risk.

Using Definition 3.6, we can express the shocked conditional mean of the systematic factor as

$$\mu_{t+h}^{(\delta_g)} = \mu_{t+h} + \psi_Z^g(h, \delta_g, \omega_{t-1}), \tag{3.22}$$

so that the closed-form GIRF of the default probability can alternatively be written directly in terms of the GIRF of the systematic factor. Substituting this expression into (3.21) yields

$$\psi^g_{\pi_i(Z)}(h, \delta_g, \omega_{t-1}) = \Phi\left(\frac{\Phi^{-1}(p_i) - \sqrt{\rho}\,(\mu_{t+h} + \psi_Z^g(h, \delta_g, \omega_{t-1}))}{\sqrt{(1-\rho) + \rho\,(s_{t+h}^{(\delta_g)})^2}}\right) - \Phi\left(\frac{\Phi^{-1}(p_i) - \sqrt{\rho}\,\mu_{t+h}}{\sqrt{(1-\rho) + \rho\,s_{t+h}^2}}\right).$$

3.2.4 Conditional mean and variance of the systemic factor

Proposition 3 shows that the GIRF of portfolio default probabilities is fully determined by the conditional mean and variance of the systematic factor, (μ_{t+h}, s_{t+h}^2), under the VAR–Merton system (3.1)–(3.5). We now detail the computation of these quantities using the lag-selection operator introduced above.

Proposition 4 (Conditional means of the systematic factor). *Under the VAR–Merton system (3.1)–(3.5), the conditional mean of the systematic factor Z_{t+h} for any horizon $h \geq 0$ is*

$$\mu_{t+h} := \mathbb{E}[Z_{t+h} \mid \Omega_{t-1}] = \beta_0 + \sum_{\ell=0}^{L_{\max}} \beta^\top S_\ell^{(s)}\, \mu_{t+h-\ell}^Y. \tag{3.23}$$

When the shock $u_t = \delta$ hits at time t, the shocked conditional mean is

$$\mu_{t+h}^{(\delta)} := \mathbb{E}[Z_{t+h} \mid u_t = \delta; \Omega_{t-1}] = \mu_{t+h} + \underbrace{\sum_{\ell=0}^{L_{\max}} \beta^\top S_\ell^{(s)}\, \Psi_{h-\ell}\, \delta}_{\psi_Z(h,\delta,\Omega_{t-1})}. \tag{3.24}$$

An analogous result applies to the conditional variances.

Proposition 5 (Conditional variances of the systematic factor). *Under the VAR–Merton system (3.1)–(3.5), the conditional variance of Z_{t+h} for any horizon $h \geq 0$ is*

$$s_{t+h}^2 := \mathrm{Var}(Z_{t+h} \mid \Omega_{t-1}) = \sum_{q=0}^{h} B(h,q)\, \Sigma_u\, B(h,q)^\top + \sigma_\eta^2. \tag{3.25}$$

Under the shock $u_t = \delta$, the conditional variance becomes

$$\left(s_{t+h}^{(\delta)}\right)^2 := \mathrm{Var}(Z_{t+h} \mid u_t = \delta; \Omega_{t-1}) = \sum_{q=1}^{h} B(h,q)\, \Sigma_u\, B(h,q)^\top + \sigma_\eta^2, \tag{3.26}$$

with σ_η^2 the variance of the error term in the satellite equation,Σ_u the variance–covariance matrix of the VAR innovations, and where

$$G_{h,q} := \sum_{\ell=0}^{L_{\max}} S_\ell^{(s)} \Psi_{h-\ell-q} \in \mathbb{R}^{m\times n}, \qquad B(h,q) := \beta^\top G_{h,q} \in \mathbb{R}^{1\times n}. \tag{3.27}$$

The proofs of Propositions 4 and 5 are provided in Appendix A.4. Combined with Proposition 3, these results allow us to fully characterise the evolution of portfolio PIT default probabilities in response to a geopolitical shock δ at time t.

Implementation. The computation can be summarised in the following pseudocode:

Algorithm 1 Computation of the GIRF of portfolio PIT default probabilities

Input: VAR estimates, shock δ, maximal horizon $h_{\max}$, coefficients β, $S_\ell^{(s)}$
Output: μ_{t+h}, $\mu_{t+h}^{(\delta)}$, s_{t+h}^2, $(s_{t+h}^{(\delta)})^2$, GIRF of PIT PDs

Compute moving–average matrices Ψ_h for $h = 0, \dots, h_{\max}$ from the companion form
Recursively compute μ_{t+h}^Y for $h = 0, \dots, h_{\max}$ using the last p observed lags of the VAR
for $h = 0$ to $h_{\max}$ **do**
    for $q = 0$ to h **do**
        Construct $G_{h,q} = \sum_{\ell=0}^{L_{\max}} S_\ell^{(s)} \Psi_{h-\ell-q}$
        Compute $B(h,q) = \beta^\top G_{h,q}$
    end for
    Compute the baseline mean μ_{t+h} using (3.23)
    Compute the shocked mean $\mu_{t+h}^{(\delta)}$ using (3.24)
    Compute the baseline variance s_{t+h}^2 using (3.25)
    Compute the shocked variance $(s_{t+h}^{(\delta)})^2$ using (3.26)
end for
Substitute these quantities into (3.2.3) to obtain the GIRF of portfolio PIT default probabilities.

4 Empirical application to U.S. credit risk

To illustrate our framework, we implement a U.S. case study.[4] A practical advantage of the VAR–Merton design is that it decouples the estimation of macroeconomic dynamics from the estimation of the credit satellite. Our macro variables cover approximately 38 years (1986:Q1–2024:Q4), whereas portfolio default rates are available for only around 9 years (2015:Q3–2024:Q4). The BVAR can therefore be estimated reliably on the long macro history, and its impulse responses can then be mapped into credit outcomes through an independently estimated Merton-style satellite. This separation makes it possible to exploit long macroeconomic histories despite short default panels, while preserving dynamic coherence and providing a transparent, closed-form link from macro shocks to portfolio PDs.

[4] Code and data: https://github.com/YoannPull/VAR-MERTON.

We proceed in three steps: (i) assess the macro effects of a GPR shock; (ii) estimate the U.S. satellite linking the systematic factor Z to selected macro covariates; and (iii) combine both blocks to obtain the horizon-by-horizon path of portfolio default probabilities (PDs) and its uncertainty. To assess robustness, we proceed in two steps. First, we re-estimate the pipeline under an alternative VAR specification while holding the default series fixed (Appendix A.7). Second, we examine sensitivity to the choice of default proxy by replacing the baseline measure with DRALACBN and replicating the analysis (Appendix A.8).

4.1 Data

This section documents the datasets used in the U.S. application: (i) the Geopolitical Risk Index (GPR), (ii) portfolio default rates from the EBA IRB panel for the United States, and (iii) a set of macro–financial time series.

4.1.1 Geopolitical risk index (GPR)

In our empirical analysis, we rely on the Geopolitical Risk Index (GPR) developed by Caldara and Iacoviello (2022) to measure both the level and the evolution of geopolitical risk over time. This index is constructed from the frequency of newspaper articles published in the United States, the United Kingdom, and Canada that report on geopolitical events. The authors justify the choice of these geographical areas by their aim to capture events with a global scope and worldwide repercussions. The evolution of the index is shown in Figure 3 below.

The construction of the index is based on a dictionary of keywords. Using terms related to war, peace, the military, nuclear issues, and terrorism, combined with expressions associated with threats ("risk," "crisis," "threat") or actions ("attack," "invasion," "bombing"), the authors build an aggregate measure of geopolitical risk (GPR). The index itself is obtained as the aggregation of two sub-indices: (i) the Geopolitical Threats Index (GPT), which captures tensions and military buildups; and (ii) the Geopolitical Acts Index (GPA), which measures the realization or escalation of adverse events. The GPR is available at a daily frequency starting in 1985.

The GPR is a particularly relevant measure of geopolitical risk for two main reasons. First, it distinguishes between the threat of a geopolitical event (tensions, sanctions, etc.) and its effective realization (war, terrorist attack). This distinction is crucial, as the mere existence of a threat, even without materialization, can influence markets and economic decisions. A bank may therefore consider scenarios that differentiate between threats and realized events in order to assess their potential impact on credit portfolios. Second, the index is not driven by macroeconomic or financial variables, such as industrial production or stock market returns. It therefore captures truly exogenous shocks that can subsequently affect the economy and financial

markets. This exogeneity has made the GPR a useful benchmark not only in academic research but also in policy discussions, as illustrated by its recent use by the European Central Bank or International Monetary Fund in their communication on geopolitical risk and financial stability Dieckelmann et al. (2024); IMF (2023).

Beyond these two key strengths, the index offers the advantage of a long historical coverage, with peaks that coincide with major geopolitical events. This allows for the replay of past episodes as well as the simulation of potential future scenarios, calibrated on historically observed fluctuations in the index. Another advantage is the possibility of decomposing the index at the country level, thereby enabling the analysis of specific regional exposures to risks that may not manifest globally.

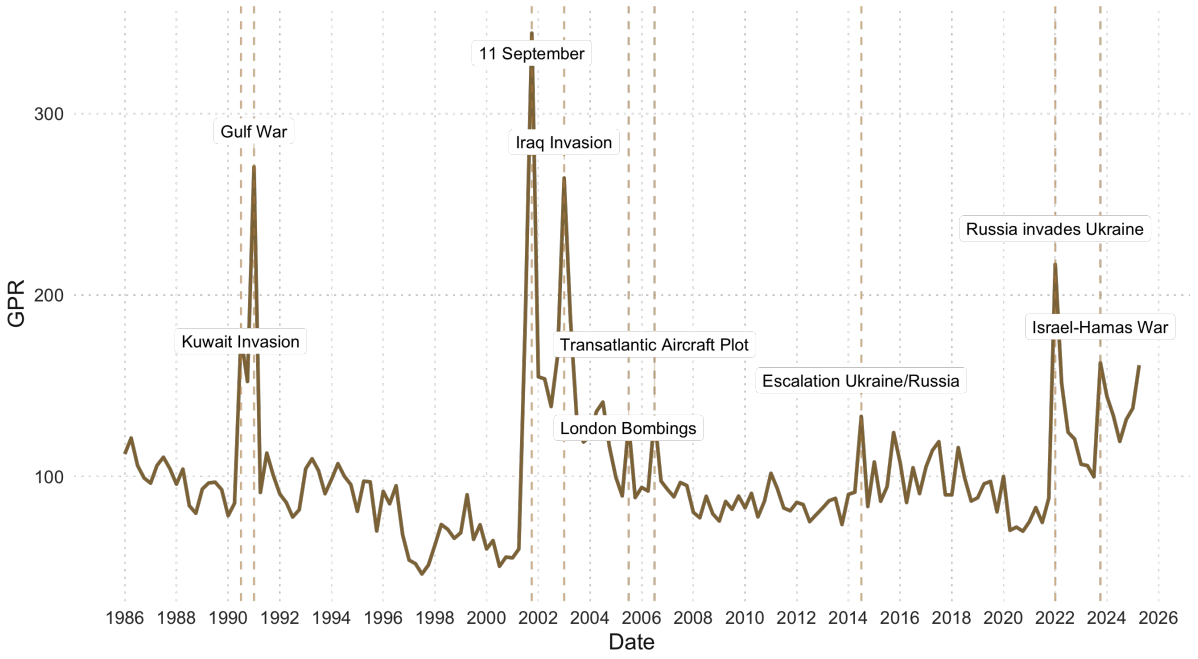

Figure 3: Geopolitical Risk Index *Notes: Quarterly averages of the Geopolitical Risk Index, covering the period from 1986:Q1 to 2024:Q4.*

4.1.2 Default data (IRB/EBA, U.S.)

The European Banking Authority (EBA) publishes aggregated historical default rates for banks using the Internal Ratings-Based (IRB) approach, at a quarterly frequency from 2015Q3 to 2024Q3, at the country level.[5] While bank-level default rates are not disclosed, the dataset reports, for each covered country and quarter, the average default rate of participating institutions together with the number of observations. For illustration, we apply our methodology to the United States subset extracted from the EBA dataset. This choice is driven by data availability;

[5] https://www.eba.europa.eu/risk-and-data-analysis/risk-analysis/risk-monitoring/risk-dashboard

the same procedure applies mutatis mutandis to other geographies where comparable information is provided. Figure 4 displays the time series of historical default rates for IRB banks in the United States, with observed values ranging from 0.4% to 1.5%. We define the Through-the-Cycle (TTC) probability of default—the unconditional PD— as the sample mean over this sample, which equals 0.79%.

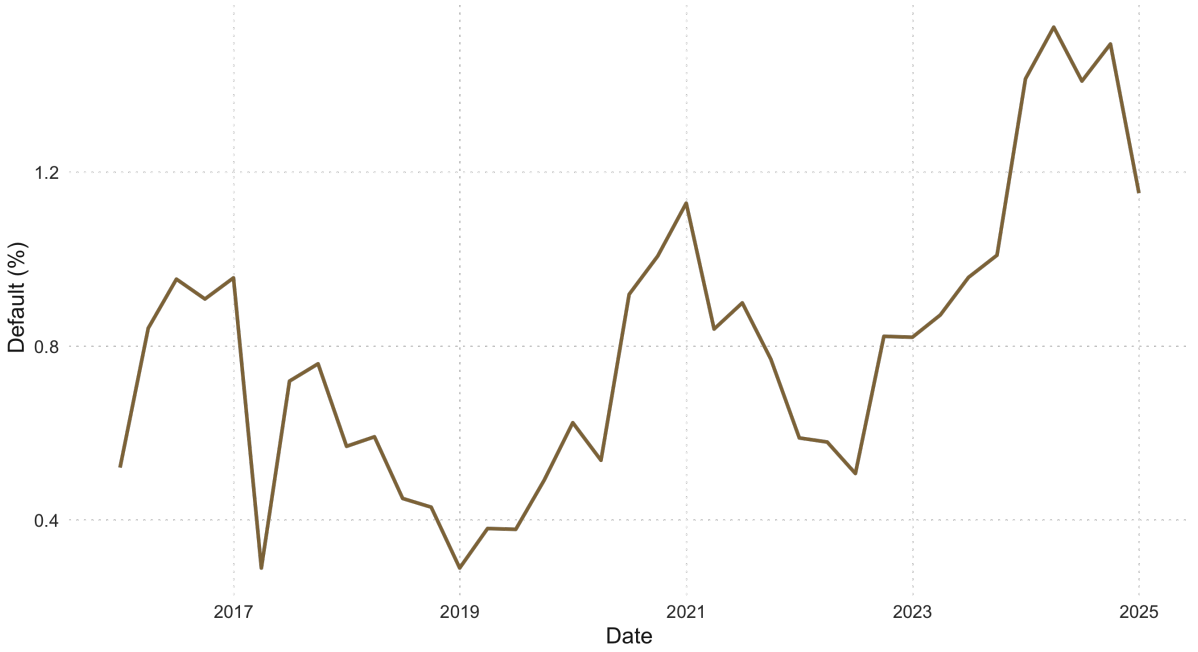

Figure 4: Historical default rates in the United States (IRB banks). *Notes: Quarterly aggregated default rates for banks applying the IRB approach in the United States (2015Q3–2024Q4).*

4.1.3 Macroeconomic and financial variables

Throughout the paper, we analyze six macro-financial time series spanning 1986Q1–2024Q4. Higher-frequency series (daily, weekly, monthly) are converted to *calendar-quarter* frequency by averaging within each quarter; series natively reported at the quarterly frequency are used as published. "Real" quantities are deflated using the Consumer Price Index for All Urban Consumers (FRED: `CPIAUCSL`). Per-capita measures divide by the civilian noninstitutional population aged 16+ (FRED: `CNP16OV`). Unless otherwise noted, logarithms are natural. Data sources and mnemonics follow the conventions below.

- **VIX** (CBOE Volatility Index; source: FRED, `VIXCLS`).
- **Log real S&P 500** (S&P 500 Composite; source: Yahoo Finance, `^GSPC` Adjusted Close; deflated by FRED `CPIAUCSL`).
- **Log real WTI oil price** (West Texas Intermediate spot; source: FRED, `WTISPLC`; deflated by FRED `CPIAUCSL`).

- **Log private hours per capita** (Nonfarm business hours; source: FRED, `HOANBS`; per capita using FRED `CNP16OV`).
- **Log real GDP per capita** (Real gross domestic product; source: FRED, `GDPC1`; per capita using FRED `CNP16OV`).
- **NFCI** (Chicago Fed National Financial Conditions Index; source: Chicago Fed / FRED, `NFCI`).

Our macro–financial block mirrors the baseline VAR specification in Caldara and Iacoviello (2022).

4.2 Results

We assess the effects of GPR shocks within the baseline VAR–Merton framework using the dataset described above. At the VAR stage, we report orthogonalized (Cholesky) impulse responses. When mapping VAR paths into the latent credit factor Z and default probabilities (PD), we compute generalized impulse responses in the sense of Koop et al. (1996). Variable definitions and code mnemonics (e.g., `log_GPRD`, `log_oil_real`) are provided in Appendix A.9.

4.2.1 VAR specification

We estimate the VAR in Section 3 on quarterly U.S. data for 1986:Q1–2024:Q4. The vector includes the geopolitical risk index (GPR) and a standard macro–financial set: real GDP per capita, total hours per capita, real oil prices, real S&P 500, the NFCI, and the VIX (log levels where indicated). Identification follows a recursive (Cholesky) scheme with GPR ordered first. Estimation is Bayesian with a Normal–Inverse–Wishart prior; we report orthogonalized IRFs to a one–s.d. GPR innovation together with pointwise 68% and 90% posterior credible bands. Robustness covering alternative VAR specifications (variable sets, identification choices) can be found in the Appendix A.5.

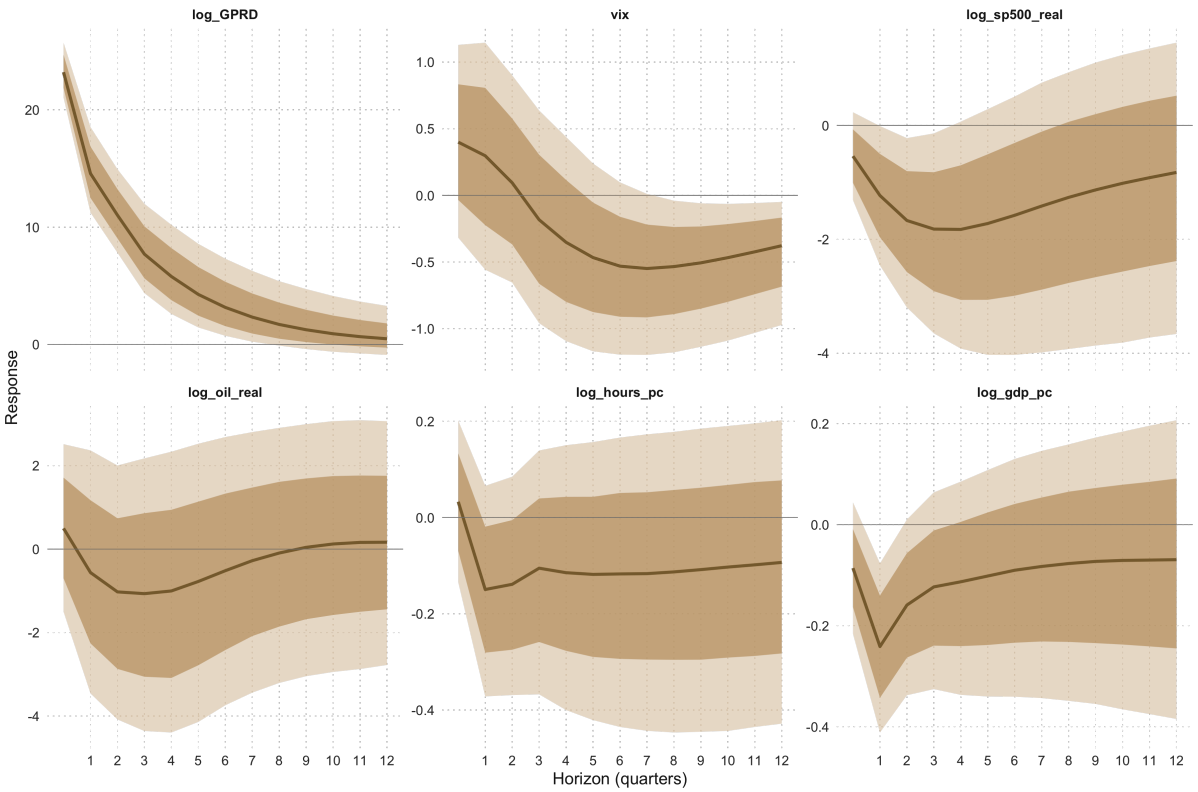

Figure 5: Macroeconomic and financial responses to a GPR shock. *Notes: Posterior medians (solid) with 68% (dark) and 90% (light) pointwise credible sets. Responses are orthogonalized (Cholesky) to a one–s.d. increase in GPR.*

Figure 5 shows a swift financial response: the VIX spikes on impact and mean–reverts; real equities (log_sp500_real) drop by about 2% at short horizons before gradually recovering; real oil prices dip temporarily. Real activity weakens—GDP per capita and hours per capita fall and remain below baseline for several quarters.

4.2.2 From macro dynamics to the systematic credit factor

We estimate the satellite in (3.5) that links the latent systematic factor Z_t to macro conditions. We follow a common variable-selection protocol : we define a candidate set of U.S. and global macro–financial covariates with lags up to p quarters, enumerate all models with at most K regressors[6], keep only those for which all coefficients are significant at the 5% level, and select the specification that minimizes AIC. This mirrors common practice for PD satellites in stress testing. Data scarcity is a common constraint in bank PD modelling: default series often span a short period and/or are observed at low frequency (quarterly), which limits the number of usable observations. Given our short PD window (37 quarterly observations, 2015:Q4–2024:Q4), we therefore report performance *in sample*. Any train/test split would leave very few observations per fold, yielding high-variance estimates and unstable selections. Robustness checks—HAC/HC3

[6]In the application below, $p = 4$ and $K = 4$.

inference—are provided in Appendix A.6.

Table 1: Determinants of the systematic factor Z (OLS).

	Estimate	Std. Error
Intercept	5.377480***	0.655721
$\log(\text{GDP pc})_{t-3}$	−0.708667***	0.100815
$\log(\text{Hours pc})_{t-3}$	0.311698***	0.081355
$\log(\text{S\&P500 real})_{t-2}$	0.096505***	0.017842
$\log(\text{Oil real})_{t-3}$	0.032275***	0.006229
Observations		37
Residual std. error		0.5726 (df = 32)
R^2 / adj. R^2		0.7086 / 0.6722
F-statistic		19.46 (4, 32)

Notes: OLS with conventional standard errors. Significance: $^{*}p < 0.10$, $^{**}p < 0.05$, $^{***}p < 0.01$.

Estimates are precise and economically interpretable: equity valuations $(t-2)$, hours per capita $(t-3)$, and real oil $(t-3)$ load positively on Z, while real GDP per capita $(t-3)$ enters with a negative sign, consistent with overlapping real-side information.

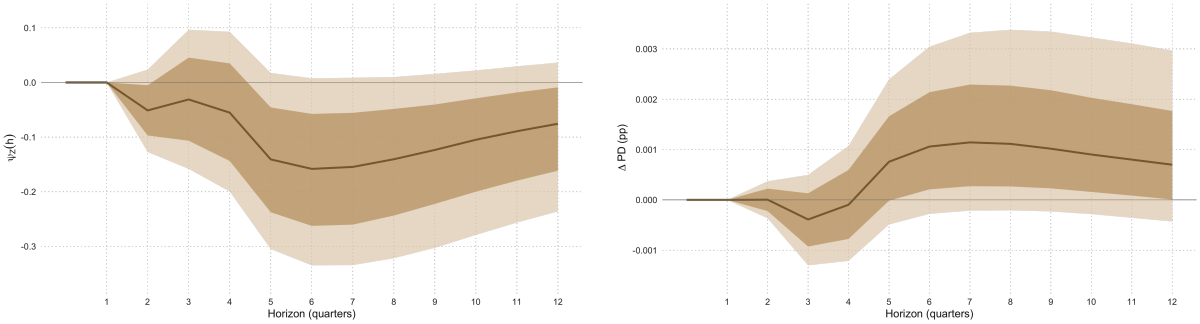

(a) Systematic factor Z (s.d.). **(b)** Portfolio PD (percentage points).

Figure 6: GIRFs to a GPR shock: Z and PD. Notes: panel (a) reports the generalized IRF of Z implied by the VAR and the satellite; panel (b) maps Z into PD via the Merton satellite. We plot the Posterior medians (solid) with 68% (dark) and 90% (light) pointwise credible sets. Responses are orthogonalized (Cholesky) to a one–s.d. increase in GPR.

Figure 6a shows the GIRF of Z to the identified GPR shock. The response is negligible on impact, turns negative within one quarter, and becomes statistically negative from $h \approx 3$. It troughs around $h = 5$–6 at roughly -0.15 s.d., then mean-reverts while remaining below baseline at the end of the horizon; bands widen with horizon, reflecting forecast uncertainty and the conditional nature of the Koop response. Figure 6b propagates the Z path through the Merton mapping (with $p = 0.79\%$ and $\rho = 0.024$), yielding a PD GIRF that is negligible on impact, turns positive after $h \approx 4$, and peaks around $h = 6$–7 at about $+0.0011$ (0.11 p.p., $\approx 14\%$ of the baseline), before mean reversion. This pattern mirrors the temporary deterioration in systematic credit conditions following a GPR shock.

4.3 Stress scenario: Replaying the past

In line with prevailing guidance, scenario design should follow the "severe yet plausible" principle: shocks must be adverse enough to expose material vulnerabilities while remaining grounded in empirical regularities and coherent economic narratives, so that results retain credibility with decision-makers, Borio et al. (2014). Consistent with this principle, we complement the one–standard-deviation experiment by replaying selected, plausibly repeatable historical episodes to benchmark magnitudes and propagation paths.

For each quarter t, we recover the innovation in the GPR equation

$$e_{\text{GPR},t} \;=\; \frac{u_{1,t}}{\sqrt{\Sigma_{1,1}}},$$

where $u_{1,t}$ is the reduced-form innovation of the (first) GPR equation and $\Sigma_{1,1}$ its instantaneous variance; thus $e_{\text{GPR},t}$ is the unit-variance Cholesky shock to GPR. In the Bayesian setup, this yields a posterior distribution for $e_{\text{GPR},t}$ at each t. Figure 7 reports posterior medians; Table 2 lists major events and their median e_{GPR}. As a concrete scenario, we calibrate the shock to the largest posterior-median innovation in our sample: 2001Q3 (September 11), with $e_{\text{GPR}} = 4.051$.[7]

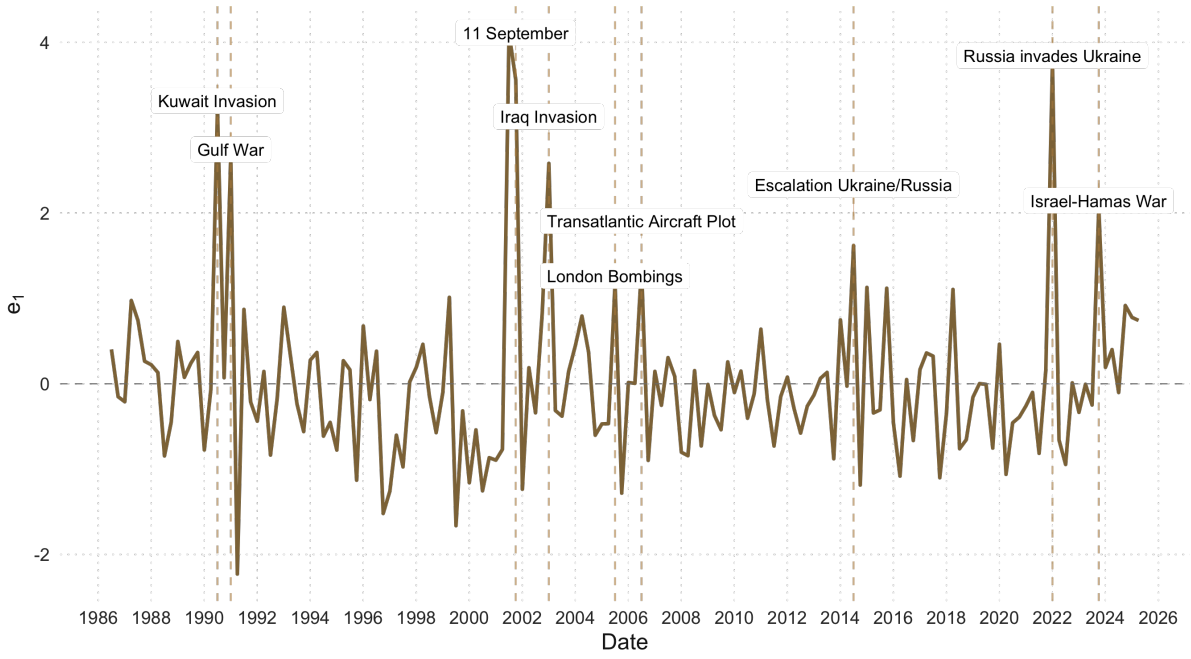

Figure 7: Innovation in GPR. *Posterior medians of $e_{GPR,t}$ across draws.*

Conditioned on a shock of this magnitude, Figure 8a shows the GIRF (Koop) of the systematic factor Z. The response is modest on impact, turns decisively negative within a few quarters, and troughs around horizons 6–8, indicating a sizable deterioration in systematic credit conditions. While credible sets widen at longer horizons, the medium-run deterioration is sharply estimated.

[7] A 4σ disturbance is extreme; lower-magnitude scenarios (e.g., 2σ) are reported in Appendix A.8 if desired.

Table 2: Major geopolitical shocks and associated e_{GPR}

Quarter	Event	Event date	GPR	e_{GPR}
1990Q3	Kuwait invasion	1990-08-02	176.641	3.234
1991Q1	Gulf War	1991-02-28	270.631	2.656
2001Q3	September 11	2001-09-11	186.559	4.051
2003Q1	Iraq invasion	2003-03-20	264.481	2.454
2005Q3	London bombings	2005-07-07	128.744	1.154
2006Q3	Transatlantic aircraft plot	2006-08-11	133.059	1.334
2014Q3	Ukraine/Russia escalation	2014-09-01	133.074	1.580
2022Q1	Russia invades Ukraine	2022-02-24	216.885	3.731
2023Q4	Israel–Hamas war	2023-10-07	162.649	2.101

Notes: e_{GPR} are the posterior-median innovations.

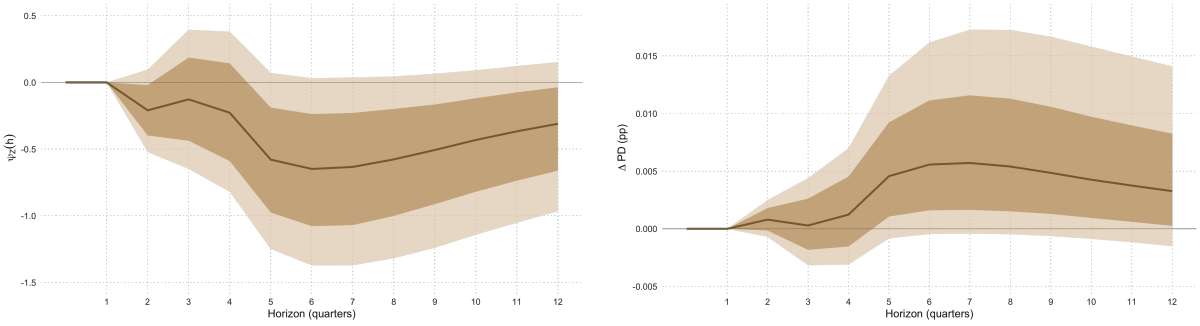

(a) Systematic factor Z (s.d.). **(b)** Portfolio PD (percentage points).

Figure 8: GIRFs under a calibrated GPR shock (2001Q3/9-11). Notes: Panel (a) displays the generalized impulse response function (IRF) of Z derived from the VAR and the satellite model. Panel (b) translates Z into the probability of default (PD) using the Merton satellite. The posterior medians are plotted as solid lines, with the 68% (dark) and 90% (light) pointwise credible intervals shown. The responses are orthogonalized (via Cholesky decomposition) to a one-standard-deviation increase in $e_{\text{GPR},t}$ of the geopolitical risk (GPR)

Figure 8b maps this dynamic into portfolio default probabilities via the Merton satellite. The PD response is negligible on impact, turns positive from $h \approx 2$, and peaks around $h \approx 7$ at +0.64 percentage points. Relative to a TTC PD of 0.79%, this corresponds to an increase of about 81%. Thereafter, PDs mean-revert but remain slightly above baseline at long horizons. Overall, a historically anchored, large GPR shock materially weakens Z and—through the nonlinear Merton mapping—translates into a sizeable yet transitory elevation in portfolio default risk.

Compared with the one–standard–deviation shock analyzed in Table 6b, the scenario response is substantially larger in magnitude and more persistent. While the baseline shock generates only a modest and short–lived increase in PD that quickly reverts toward zero, the 9/11 scenario amplifies the effect by nearly an order of magnitude and sustains it over several quarters, highlighting the nonlinear amplification of extreme geopolitical events on portfolio credit risk.

5 Conclusion

We develop a coherent macro-to-credit pipeline that traces the effect of exogenous geopolitical risk shocks on U.S. bank default risk. A recursively identified VAR provides internally consistent macro-financial impulse paths; a Merton satellite converts the implied trajectory of the systematic factor into portfolio PD dynamics, with a closed-form expression for generalized impulse responses. In our application (1986:Q1–2024:Q4 macro; 2015:Q3–2024:Q4 defaults), a typical GPR shock raises market volatility on impact, depresses equities at short horizons, lowers the systematic factor by about 0.15 s.d. at 5–6 quarters, and increases PD by roughly 0.11 pp (14% of a 0.80% baseline) at 6–7 quarters before mean reversion.

Relative to *EBA-stress-testing*, the framework is an *applied methodological advancement*: it preserves the usability and comparability of published scenarios while adding dynamic coherence and an analytic, transparent macro-to-PD bridge. Governance and standardization remain important—priors and identification choices should be disclosed and benchmarked—but the approach is tractable, replicable and directly portable to policy use.

Ultimately, this two-step methodology provides a structured framework enabling banks to assess geopolitical risk and conduct internal stress tests to evaluate the vulnerability of their credit portfolios to a geopolitical shock. It contributes directly to addressing Priority 1 set by the ECB's banking supervision for the 2024–2026 period, which aims to strengthen resilience to immediate macro-financial and geopolitical shocks, including their impact on credit risk.

Unlike climate risk, no reference scenarios currently exist for the occurrence of a geopolitical shock, due to its unpredictable nature and the multiplicity of potential effects, as Buch (2024) points out. The first step of our methodology allows, conditional on a shock, the assessment of impacts on macroeconomic factors used in credit risk models, thus providing an alternative in the absence of reference scenarios. The second step, through impulse response function analysis, enables the estimation of the consequences of these shocks on the economy and, by extension, on credit portfolios. Consequently, our methodological framework could also be applied to climate risk or other emerging risks, provided that reference scenarios exist, such as those proposed by the NGFS or supplied by regulators during stress-testing exercises.

Two extensions appear particularly promising. First, building on Faria-e Castro and Leibovici (2024), advances in artificial intelligence could help generate synthetic news narratives for plausible geopolitical events, which could then be mapped into a projected GPR path and an associated shock; the implied impacts on macro variables and portfolio PDs would follow directly from our pipeline. Second, the framework could be adapted to a reverse stress testing use case:

starting from a pre-defined breakdown outcome (e.g., CET1 depletion or a critical increase in portfolio PD), it would back out the magnitude and propagation of a geopolitical shock—and the corresponding macro-financial paths—consistent with reaching that threshold. We expect this direction to be particularly relevant given the ECB's planned 2026 geopolitical risk reverse stress test for 110 significant institutions European Central Bank (2025).

References

Abadie, A. and Gardeazabal, J. (2003). The economic costs of conflict: A case study of the basque country. *American Economic Review*, 93(1):113–132.

Adrian, M. T., Morsink, M. J., and Schumacher, M. B. (2020). *Stress Testing at the IMF*. International Monetary Fund.

AXA (2024). Future risks report 2024. 11th edition.

Baker, S. R., Bloom, N., and Davis, S. J. (2016). Measuring economic policy uncertainty. *The Quarterly Journal of Economics*, 131(4):1593–1636.

Bank of England (2024). System-wide exploratory scenario: Final system-wide results. Technical report, Bank of England.

Behn, M., Lang, J. H., and Reghezza, A. (2025). 120 years of insight: Geopolitical risk and bank solvency. *Economics Letters*, 247:112168.

Belkin, B., Suchower, S., and Forest, L. (1998). A one-parameter representation of credit risk and transition matrices. *CreditMetrics monitor*, 1(3):46–56.

Blattman, C. and Miguel, E. (2010). Civil war. *Journal of Economic Literature*, 48(1):3–57.

Blomberg, S. B., Hess, G. D., and Orphanides, A. (2004). The macroeconomic consequences of terrorism. *Journal of Monetary Economics*, 51(5):1007–1032.

Board of Governors of the Federal Reserve System (2025). 2025 supervisory scenarios for annual stress tests. Technical report, Federal Reserve.

Borio, C., Drehmann, M., and Tsatsaronis, K. (2014). Stress-testing macro stress testing: does it live up to expectations? *Journal of Financial Stability*, 12:3–15.

Bouras, C., Christou, C., Gupta, R., and Suleman, T. (2019). Geopolitical risks, returns, and volatility in emerging stock markets: Evidence from a panel GARCH model. *Emerging Markets Finance and Trade*, 55(8):1841–1856.

Buch, C. (2024). Global rifts and financial shifts: supervising banks in an era of geopolitical instability. Keynote speech at the ESRB annual conference.

Budnik, K., Ponte Marques, R., Ben Hadj, Y., Georgescu, O., Giglio, S., Grassi, S., Durrani, A., Figueres, J., Konietschke, S., Le Grand, F., Metzler, P., Ortl, T., Población García, J., Shaw,

K., Trachana, G., Chalf, M., Gross, M., Sydow, M., and Franch, F. (2024). Advancements in stress-testing methodologies for financial stability applications. ECB Occasional Paper Series 348, European Central Bank.

Caldara, D. and Iacoviello, M. (2022). Measuring geopolitical risk. *American Economic Review*, 112(4):1194–1225.

Choudhry, T. (2010). World War II events and the dow jones industrial index. *Journal of Banking & Finance*, 34(5):1022–1031.

Dieckelmann, D., Kaufmann, C., Larkou, C., McQuade, P., Negri, C., Pancaro, C., and Rößler, D. (2024). Turbulent times: geopolitical risk and its impact on euro area financial stability. *Financial Stability Review*, 1.

ECB (2025). Financial Stability Review, Overview, May 2025.

Eckstein, Z. and Tsiddon, D. (2004). Macroeconomic consequences of terror: Theory and the case of Israel. *Journal of Monetary Economics*, 51(5):971–1002.

Engle, R. F. and Campos-Martins, S. (2023). What are the events that shake our world? Measuring and hedging global COVOL. *Journal of Financial Economics*, 147(1):221–242.

European Banking Authority (2025). Methodological note for the 2025 eu-wide stress test. Technical report, EBA.

European Central Bank (2025). ECB to assess banks' stress testing capabilities to capture geopolitical risk. https://www.bankingsupervision.europa.eu/press/pr/date/2025/html/ssm.pr251212~69f656d4bf.en.html. ECB Banking Supervision press release, 12 December 2025 (accessed 15 January 2026).

Faria-e Castro, M. and Leibovici, F. (2024). Artificial intelligence and inflation forecasts. *Federal Reserve Bank of St. Louis Review*, 106(12):1–14.

Glick, R. and Taylor, A. M. (2010). Collateral damage: Trade disruption and the economic impact of war. *Review of Economics and Statistics*, 92(1):102–127.

Gouriéroux, C. and Tiomo, A. (2007). *Risque de crédit: une approche avancée*. Economica.

Henry, J. and Kok, C. (2013). A macro stress testing framework for assessing systemic risks in the banking sector. In Fouque, J.-P. and Langsam, J. A., editors, *Handbook of Systemic Risk*, pages 619–640. Cambridge University Press.

IMF (2023). Global financial stability report: Safeguarding financial stability amid high inflation and geopolitical risks. International Monetary Fund.

Koop, G., Pesaran, M. H., and Potter, S. M. (1996). Impulse response analysis in nonlinear multivariate models. *Journal of Econometrics*, 74(1):119–147.

Merton, R. C. (1974). On the pricing of corporate debt: The risk structure of interest rates. *The Journal of Finance*, 29(2):449–470.

Nguyen, T. C. and Thuy, T. H. (2023). Geopolitical risk and the cost of bank loans. *Finance Research Letters*, 54:103812.

Pesaran, M. H. and Shin, Y. (1998). Generalized impulse response analysis in linear multivariate models. *Economics Letters*, 58(1):17–29.

Phan, D. H. B., Tran, V. T., and Iyke, B. N. (2022). Geopolitical risk and bank stability. *Finance Research Letters*, 46:102453.

Pinchetti, M. (2025). Geopolitical risk and inflation: The role of energy markets. Working Paper 1005, Banque de France.

Quagliariello, M. (2009). *Stress-testing the Banking System: Methodologies and Applications*. Cambridge University Press, Cambridge.

Rigobon, R. and Sack, B. (2005). The effects of war risk on US financial markets. *Journal of Banking & Finance*, 29(7):1769–1789.

Shawon, R. E. R., Dalim, H. M., Shil, S. K., Gurung, N., Hasanuzzaman, M., Hossain, S., and Rahman, T. (2024). Assessing geopolitical risks and their economic impact on the USA using data analytics. *Journal of Economics, Finance and Accounting Studies*, 6(6):05–16.

Umar, Z., Bossman, A., Choi, S.-Y., and Teplova, T. (2022). Does geopolitical risk matter for global asset returns? evidence from quantile-on-quantile regression. *Finance Research Letters*, 48:102991.

Vasicek, O. (2002). The distribution of loan portfolio value. *Risk*, 15(12):160–162.

Wang, Y., Song, G., and Lu, Y. (2025). Geopolitical risk, bank regulation, and systemic risk: A cross-country analysis. *Finance Research Letters*, 76:106893.

Wei, J., Chen, W.-Q., Chen, C., Huang, Y., and Tang, L. (2024). Evaluating the bulk commodities supply risk from the perspective of physical trade. *Resources Policy*, 93:105059.

World Economic Forum (2025). Global risks report 2025. June 2025.

Zhu, S., Xia, Y., Li, Q., and Chen, Y. (2025). Global geopolitical risk and financial stability: Evidence from china. *Finance Research Letters*, 72:106501.

A Appendices

A.1 Proof of Proposition 1

Proof. By the definition of $Y_t^{(s)}$,

$$Y_{t+h}^{(s)} \;=\; \sum_{\ell=0}^{L_{\max}} S_\ell^{(s)}\, Y_{t+h-\ell}. \tag{A.1}$$

Taking conditional expectations and using the linearity of each $S_\ell^{(s)}$,

$$\mathbb{E}[\, Y_{t+h}^{(s)} \mid u_t = \delta,\, \Omega_{t-1} = \omega_{t-1}] = \sum_{\ell=0}^{L_{\max}} S_\ell^{(s)}\, \mathbb{E}[\, Y_{t+h-\ell} \mid u_t = \delta,\, \Omega_{t-1} = \omega_{t-1}]. \tag{A.2}$$

An analogous expression holds without the imposed shock. Subtracting the two conditional expectations term by term gives

$$\psi_{Y^{(s)}}(h, \delta, \omega_{t-1}) = \sum_{\ell=0}^{L_{\max}} S_\ell^{(s)} \Big(\mathbb{E}[Y_{t+h-\ell} \mid u_t = \delta,\, \Omega_{t-1}{=}\omega_{t-1}] - \mathbb{E}[Y_{t+h-\ell} \mid \Omega_{t-1}{=}\omega_{t-1}]\Big).$$

which is exactly $\sum_{\ell=0}^{L_{\max}} S_\ell^{(s)}\, \psi_Y(h-\ell, \delta, \omega_{t-1})$, with the convention $\psi_Y(h', \cdot, \cdot) \equiv 0$ for $h' < 0$. This proves (3.15). □

A.2 Proof of Lemma 1

Proof. Let $V \sim \mathcal{N}(0,1)$ be independent of W, and define $U := \sqrt{\rho}\, W + \sqrt{1-\rho}\, V$. Then,

$$\Phi\left(\frac{\Phi^{-1}(p) - \sqrt{\rho}\, W}{\sqrt{1-\rho}}\right) = \Pr\left(V \le \frac{\Phi^{-1}(p) - \sqrt{\rho}\, W}{\sqrt{1-\rho}} \,\middle|\, W\right) = \Pr(U \le \Phi^{-1}(p) \,|\, W). \tag{A.3}$$

Taking expectations and applying the law of iterated expectations,

$$\mathbb{E}\left[\Phi\left(\frac{\Phi^{-1}(p) - \sqrt{\rho}\, W}{\sqrt{1-\rho}}\right)\right] = \mathbb{E}\Big[\Pr(U \le \Phi^{-1}(p) \,|\, W)\Big] = \Pr(U \le \Phi^{-1}(p)). \tag{A.4}$$

Since $W \sim \mathcal{N}(\mu, \sigma^2)$ and $V \sim \mathcal{N}(0,1)$ are independent, we have $U \sim \mathcal{N}(\sqrt{\rho}\,\mu,\ (1-\rho) + \rho\,\sigma^2)$. Therefore,

$$\Pr(U \le \Phi^{-1}(p)) = \Phi\left(\frac{\Phi^{-1}(p) - \sqrt{\rho}\,\mu}{\sqrt{(1-\rho) + \rho\,\sigma^2}}\right), \tag{A.5}$$

which proves (3.18). □

A.3 Proof of Proposition 3

Proof. Conditional on $Y_{t+h}^{(s)}$, we have

$$(Z_{t+h} \mid Y_{t+h}^{(s)}) \sim \mathcal{N}(\beta_0 + \beta^\top Y_{t+h}^{(s)},\ \sigma_\eta^2). \tag{A.6}$$

Under the Gaussian VAR, both $(Y_{t+h}^{(s)} \mid \omega_{t-1})$ and $(Y_{t+h}^{(s)} \mid u_t = \delta; \omega_{t-1})$ are Gaussian; Gaussian integration then yields

$$(Z_{t+h} \mid \omega_{t-1}) \sim \mathcal{N}(\mu_{t+h}, s_{t+h}^2) \tag{A.7}$$

and

$$(Z_{t+h} \mid u_t = \delta; \omega_{t-1}) \sim \mathcal{N}(\mu_{t+h}^{(\delta)}, (s_{t+h}^{(\delta)})^2). \tag{A.8}$$

Equation (3.21) follows from Lemma 1 applied to the two distributions. □

A.4 Proof of Propositions 4 and 5

Proof. Let $\{\Psi_h\}_{h\geq 0}$ denote the moving–average coefficient matrices of the VAR, so that for any horizon $r \geq 0$,

$$Y_{t+r} \;=\; \mu_{t+r}^{Y} \;+\; \sum_{q=0}^{r} \Psi_{r-q}\, u_{t+q}, \qquad \Psi_0 = I_n, \tag{A.9}$$

where μ_t^Y denotes the baseline VAR forecast computed recursively from the last p observed lags. We adopt the convention that $\Psi_r \equiv 0$ and $\mu_{t+r}^Y \equiv 0$ for $r < 0$.

Let $S^{(s)}(L) = \sum_{\ell=0}^{L_{\max}} S_\ell^{(s)} L^\ell$ be the polynomial selection operator of Definition 3, so that

$$Y_t^{(s)} \;=\; \sum_{\ell=0}^{L_{\max}} S_\ell^{(s)}\, Y_{t-\ell}. \tag{A.10}$$

The satellite equation is linear:

$$Z_t \;=\; \beta_0 \;+\; \beta^\top Y_t^{(s)} \;+\; \eta_t, \qquad \eta_t \sim \mathcal{N}(0, \sigma_\eta^2), \quad \eta_t \perp\!\!\!\perp \{u_s\}_{s\in\mathbb{Z}}. \tag{A.11}$$

Mean path. By iterated expectations and linearity, for any $h \geq 0$,

$$\mu_{t+h} \;:=\; \mathbb{E}[Z_{t+h} \mid \omega_{t-1}] \;=\; \beta_0 \;+\; \beta^\top \mathbb{E}\Big[Y_{t+h}^{(s)} \mid \omega_{t-1}\Big], \tag{A.12}$$

and, using the definition of $Y_{t+h}^{(s)}$ and the fact that $\mathbb{E}[Y_{t+h-\ell} \mid \omega_{t-1}] = \mu_{t+h-\ell}^Y$,

$$\mathbb{E}\Big[Y_{t+h}^{(s)} \mid \omega_{t-1}\Big] \;=\; \sum_{\ell=0}^{L_{\max}} S_\ell^{(s)}\, \mu_{t+h-\ell}^{Y}. \tag{A.13}$$

Hence

$$\mu_{t+h} \;=\; \beta_0 \;+\; \sum_{\ell=0}^{L_{\max}} \beta^\top S_\ell^{(s)}\, \mu_{t+h-\ell}^{Y}, \tag{A.14}$$

which is (3.23).

Under a GIRF à la Koop et al. (1996) with a realized reduced–form shock $u_t = \delta$ at date t, the conditional mean of Z_{t+h} satisfies

$$\mu_{t+h}^{(\delta)} \;:=\; \mathbb{E}[Z_{t+h} \mid u_t = \delta;\, \omega_{t-1}] \;=\; \mu_{t+h} \;+\; \psi_Z(h, \delta, \omega_{t-1}), \tag{A.15}$$

by the definition of the GIRF for Z_{t+h} (see Proposition 2). Moreover, Proposition 2 implies that the GIRF of the VAR state satisfies

$$\psi_Y(h, \delta, \omega_{t-1}) \;=\; \Psi_h\, \delta, \tag{A.16}$$

so that the GIRF of the satellite variable is obtained by propagating this response through the linear satellite equation and the selection operator. This yields

$$\psi_Z(h,\delta,\omega_{t-1}) \;=\; \sum_{\ell=0}^{L_{\max}} \beta^\top S_\ell^{(s)} \Psi_{h-\ell}\,\delta, \tag{A.17}$$

which, combined with the previous display, gives

$$\mu_{t+h}^{(\delta)} \;=\; \mu_{t+h} \;+\; \sum_{\ell=0}^{L_{\max}} \beta^\top S_\ell^{(s)} \Psi_{h-\ell}\,\delta, \tag{A.18}$$

that is (3.24). This proves Proposition 4.

Variance path. Using the moving–average representation of Y_{t+h} in the selected block, we obtain

$$\begin{aligned} Y_{t+h}^{(s)} \;&=\; \sum_{\ell=0}^{L_{\max}} S_\ell^{(s)} Y_{t+h-\ell} \\ &=\; \sum_{\ell=0}^{L_{\max}} S_\ell^{(s)} \mu_{t+h-\ell}^{Y} \;+\; \sum_{\ell=0}^{L_{\max}} S_\ell^{(s)} \Big(\sum_{q=0}^{h-\ell} \Psi_{h-\ell-q} u_{t+q} \Big). \end{aligned} \tag{A.19}$$

Reordering the double sum over (ℓ, q) and using the convention $\Psi_r \equiv 0$ for $r < 0$, we may write

$$Y_{t+h}^{(s)} \;=\; \sum_{\ell=0}^{L_{\max}} S_\ell^{(s)} \mu_{t+h-\ell}^{Y} \;+\; \sum_{q=0}^{h} \Big(\sum_{\ell=0}^{L_{\max}} S_\ell^{(s)} \Psi_{h-\ell-q} \Big) u_{t+q}. \tag{A.20}$$

By definition of $G_{h,q}$ in (3.27), this is

$$Y_{t+h}^{(s)} \;=\; \sum_{\ell=0}^{L_{\max}} S_\ell^{(s)} \mu_{t+h-\ell}^{Y} \;+\; \sum_{q=0}^{h} G_{h,q}\, u_{t+q}. \tag{A.21}$$

Substituting into the satellite equation at horizon $t+h$ gives

$$\begin{aligned} Z_{t+h} \;&=\; \beta_0 \;+\; \beta^\top Y_{t+h}^{(s)} \;+\; \eta_{t+h} \\ &=\; \beta_0 \;+\; \sum_{\ell=0}^{L_{\max}} \beta^\top S_\ell^{(s)} \mu_{t+h-\ell}^{Y} \;+\; \sum_{q=0}^{h} \beta^\top G_{h,q}\, u_{t+q} \;+\; \eta_{t+h}. \end{aligned} \tag{A.22}$$

Using the definition $B(h,q) := \beta^\top G_{h,q}$ in (3.27), and the expression for μ_{t+h} in (3.23), we obtain

$$Z_{t+h} - \mu_{t+h} \;=\; \sum_{q=0}^{h} B(h,q)\, u_{t+q} \;+\; \eta_{t+h}. \tag{A.23}$$

Assuming $\mathrm{Var}(u_t) = \Sigma_u$ and that $\{u_t\}$ is serially uncorrelated and independent of η_{t+h}, it follows that

$$\begin{aligned} s_{t+h}^2 \;:=\; \mathrm{Var}(Z_{t+h} \mid \omega_{t-1}) \;&=\; \mathrm{Var}\Big(\sum_{q=0}^{h} B(h,q)\, u_{t+q} \;+\; \eta_{t+h} \,\Big|\, \omega_{t-1} \Big) \\ &=\; \sum_{q=0}^{h} B(h,q)\, \Sigma_u\, B(h,q)^\top \;+\; \sigma_\eta^2, \end{aligned} \tag{A.24}$$

which is (3.25).

Under a GIRF à la Koop et al. (1996), we condition on $u_t = \delta$, so that u_t is treated as non–random in the conditional distribution of Z_{t+h}. Hence the $q = 0$ term in the variance drops out, while all terms with $q \geq 1$ remain stochastic. Therefore,

$$\begin{aligned}\left(s_{t+h}^{(\delta)}\right)^2 \;:=\; \mathrm{Var}(Z_{t+h} \mid u_t = \delta;\, \omega_{t-1}) \;&=\; \mathrm{Var}\Big(\sum_{q=1}^{h} B(h,q)\, u_{t+q} \;+\; \eta_{t+h} \,\Big|\, u_t = \delta;\, \omega_{t-1}\Big) \\ &= \sum_{q=1}^{h} B(h,q)\, \Sigma_u\, B(h,q)^\top \;+\; \sigma_\eta^2,\end{aligned} \tag{A.25}$$

which is (3.26). This establishes Proposition 5 and completes the proof. □

A.5 VAR Specifications

This appendix reports ten alternative Vector Autoregression (VAR) specifications, listed in Table 3, which are employed to assess the robustness of the results to different macro–financial information sets. The lag length is fixed at $p = 2$, and identification relies on a recursive (Cholesky) scheme with `log_GPRD` placed first in the ordering. Definitions of the variables and their code mnemonics (e.g., `log_GPRD`, `log_oil_real`) are provided in Appendix A.9.

Table 3: Specifications tested (VAR; recursive/Cholesky ordering)

Spec	$k-1$	**Variables (in addition to `log_GPRD`; shock order)**
S1_baseline	6	vix, log_sp500_real, log_oil_real, log_hours_pc, log_gdp_pc
S2_appendix	6	vix, log_sp500_real, gs2, log_inv_pc, log_gdp_pc, log_hours_pc
S3	6	vix, log_sp500_real, log_oil_real, log_inv_pc, log_gdp_pc, log_hours_pc
S4	6	vix, nfci, epu, log_sp500_real, gs2, log_gdp_pc
S5	5	log_inv_pc, log_gdp_pc, log_hours_pc, log_oil_real, infl_yoy_pct
S6	6	vix, log_sp500_real, gs2, t10Y3M, nfci, epu
S7	5	gdp_yoy_pct, infl_annualized_pct, log_oil_real, vix, log_sp500_real
S8	4	vix, log_sp500_real, log_oil_real, log_gdp_pc

Notes: $k-1$ counts variables in addition to `log_GPRD`.
Variables are listed in the **shock order**, from most "exogenous" (left) to most "endogenous" (right).
`log_GPRD` is always **first** and receives the shock.

Posterior inference relies on a conjugate Normal–Inverse–Wishart prior with 20,000 draws per specification. For transparency, we report on Table 4 (i) the fraction of posterior draws that are dynamically stable (spectral radius of the companion matrix < 1) and (ii) the median and 95th percentile of the largest-modulus eigenvalue. Orthogonalized impulse responses (OIRFs) to a one–standard deviation shock in `log_GPRD` are computed over horizons $h = 0, \ldots, 12$ and summarized by the posterior median with 68% and 90% credible bands.

Across the eight specifications ($k = 5$–7), the share of stable draws is close to 0.60 for most models (S1_baseline = 0.513, S2_appendix = 0.536, S3 = 0.551, S7 = 0.610, S8 = 0.622) and peaks for the spreads-based S5 (= 0.622). Two financially tight variants (S4 with NFCI/EPU and S6 financial-only) display low stability (0.139 and 0.187). The companion-matrix spectral radius is close to but below unity in all cases (median $|\lambda|_{\max} \in [0.989, 0.996]$, 95th percentile up to 0.9996), indicating models near the stationarity boundary. Interpretation therefore focuses on the eight specifications with stability ≥ 0.5.

Table 4: Posterior stability diagnostics and outputs (BVAR, NIW prior)

Spec	k	p	Draws n	Stable share	Stable n	$\lvert\lambda\rvert_{\max}$ median	$\lvert\lambda\rvert_{\max}$ p95
S1_baseline	7	2	20 000	0.5132	10 263	0.9958	0.9996
S2_appendix	7	2	20 000	0.5355	10 710	0.9952	0.9995
S3	7	2	20 000	0.5508	11 016	0.9955	0.9995
S4	7	2	20 000	0.1392	2783	0.9942	0.9995
S5	6	2	20 000	0.6220	12 439	0.9956	0.9995
S6	7	2	20 000	0.1867	3734	0.9901	0.9992
S7	6	2	20 000	0.6104	12 209	0.9891	0.9990
S8	5	2	20 000	0.6218	12 437	0.9929	0.9993

Notes: k is the number of variables (including `log_GPRD`); p is the VAR lag order. "Stable share" is the fraction of posterior draws with spectral radius < 1. $|\lambda|_{\max}$ is the largest-modulus eigenvalue of the companion matrix. Credible IRF bands use quantiles {5%, 16%, 50%, 84%, 95%}.

A.6 Robust inference (HAC and HC3) for the estimation of Z

We re-estimate the baseline OLS satellite for Z_t (Table 1) using (i) Newey–West HAC standard errors with prewhitening and lag = 4, and (ii) heteroskedasticity-robust HC3 (MacKinnon–White). Point estimates are unchanged; only the covariance matrix varies. Signs and magnitudes are stable across estimators, and all slopes remain statistically significant (at least at the 1% level). Table 5 and 6 show the results.

Table 5: Satellite Z: robust inference with HAC (Newey–West).

Variable	**Estimate**	**Std. Error**
Intercept	-5.377480***	22.513
$\log(\text{GDP pc})_{t-3}$	-0.70867***	0.091674
$\log(\text{Hours pc})_{t-3}$	0.31170***	0.078595
$\log(\text{S\&P500 real})_{t-2}$	0.096504***	0.018129
$\log(\text{Oil real})_{t-3}$	0.032274***	0.006925

Notes: HAC = Newey–West with prewhitening, lag = 4, and d.f. adjustment. OLS point estimates are identical to Table 1. Significance: * $p < 0.05$, ** $p < 0.01$, *** $p < 0.001$.

Table 6: Satellite Z: robust inference with HC3.

Variable	Estimate	Std. Error
Intercept	-5.377480***	22.780
$\log(\text{GDP pc})_{t-3}$	-0.70867***	0.090728
$\log(\text{Hours pc})_{t-3}$	0.31170**	0.090682
$\log(\text{S\&P500 real})_{t-2}$	0.096504***	0.017543
$\log(\text{Oil real})_{t-3}$	0.032274***	0.006985

Notes: HC3 = heteroskedasticity-robust (MacKinnon–White). OLS point estimates are identical to Table 1. Significance: * $p < 0.05$, ** $p < 0.01$, *** $p < 0.001$.

We also report in Table 7 the 6 top coefficients obtained from the Lasso regression for the selected variables. The variables are ordered by the absolute value of their coefficients. The Lasso model was fitted using cross-validation to select the optimal regularization parameter λ. Cross-validation helps ensure that the selected λ is robust by evaluating the model's performance on multiple subsets of the data, thereby reducing the risk of overfitting.

When comparing these results with the OLS model in Table 1, we observe that both models identify similar variables as important predictors of the systematic factor Z, such as $\log(\text{GDP pc})_{t-3}$ and $\log(\text{Hours pc})_{t-3}$. However, while the Lasso model selects more moderate values and forces some coefficients to zero, the OLS model estimates non-zero coefficients with more variability. In particular, the Lasso coefficients are generally smaller in magnitude, reflecting the regularization. Both models suggest that variables like $\log(\text{GDP pc})_{t-3}$ have a negative relationship with Z, while $\log(\text{Hours pc})_{t-3}$ and $\log(\text{VIX})_t$ exhibit positive relationships.

Table 7: Lasso Regression Results: Top 6 Coefficients for Selected Variables.

Variable	Estimate
Intercept	4.5401
$\log(\text{GDP pc})_{t-3}$	-0.23462
$\log(\text{GDP pc})_{t-1}$	-0.05233
$\log(\text{Hours pc})_{t-3}$	0.06690
$\log(\text{VIX})_t$	0.05277
$\log(\text{Oil real})_{t-0}$	0.01488
$\log(\text{S\&P500 real})_{t-0}$	0.01905
Observations	37
R^2	0.7658
Optimal λ	0.01953
Validation Method	Cross-Validation (Mean Squared Error)

Notes: The table reports the coefficients obtained from the Lasso regression for the top 6 variables selected based on the absolute value of their coefficients. The optimal λ was selected using cross-validation based on Mean Squared Error. The "Top 6" refers to the six variables with the largest absolute coefficients, which were considered the most influential in the model.

A.7 Alternative identification schemes for the VAR: effects on default probabilities

To assess robustness, we select one of the best/performing VAR specifications in terms of the fraction of draws that satisfy the stability condition (all roots outside the unit circle) reported in Table 4, with an emphasis on parsimoniously capturing macroeconomic dynamics. Identification follows a recursive (Cholesky) scheme with the ordering

$$S5 : (\log GPRD,\ \log inv\_pc,\ \log gdp\_pc,\ \log hours\_pc,\ \log oil\_real,\ infl\_yoy\_pct).$$

This ordering is economically coherent for quarterly data: (i) geopolitical risk ($GPRD$) is treated as contemporaneously exogenous to domestic macroeconomic conditions; (ii) investment typically reacts within the quarter to uncertainty and financial conditions and thus precedes output; (iii) hours adjust after output because of labor/market frictions; (iv) the real price of oil is allowed to respond contemporaneously to demand conditions—proxied by activity—while transmitting to prices with a delay; and (v) inflation (year/over/year) is placed last so it can respond contemporaneously to all real shocks and to oil. Figures 9 show the IRF to a one-s.d increase in GPR.

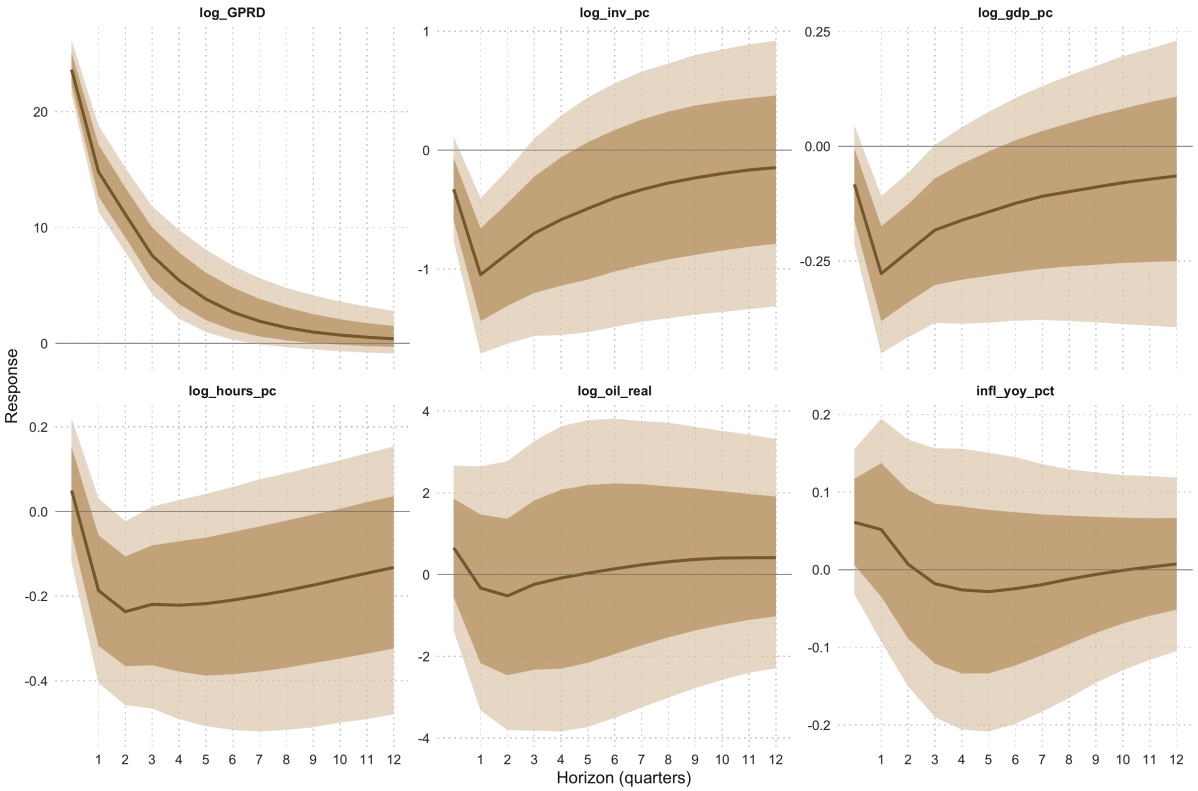

Figure 9: Macroeconomic responses to a GPR shock of the S6 specification *Notes: Posterior medians (solid) with 68% (dark) and 90% (light) pointwise credible sets. Responses are orthogonalized (Cholesky) to a one–s.d. increase in GPR.*

Using the VAR variable set, we estimate alternative linear models for the systematic factor Z;

the preferred specification—selected by the lowest AIC among valid candidates—is reported in Table 8.

Table 8: Determinants of the systematic factor Z (OLS).

	Estimate	Std. Error
Intercept	2.267089***	8.607230
$\log(\text{Investment pc})_{t-1}$	0.154327*	0.064367
$\log(\text{GDP pc})_{t-1}$	−0.419907***	0.093988
$\log(\text{Oil real})_{t-1}$	0.026471***	0.007074
Selection criterion	Lowest AIC among valid models	
AIC (selected model)		79.741
Observations		37
Residual std. error		0.6575 (df = 33)
R^2 / adj. R^2		0.6038 / 0.5677
F-statistic		16.76 (3, 33)

Notes: Dependent variable is standardized Z. OLS with conventional standard errors. Significance: $^{*}p < 0.10$, $^{**}p < 0.05$, $^{***}p < 0.01$. Model F-statistic p-value: 8.619×10^{-7}.

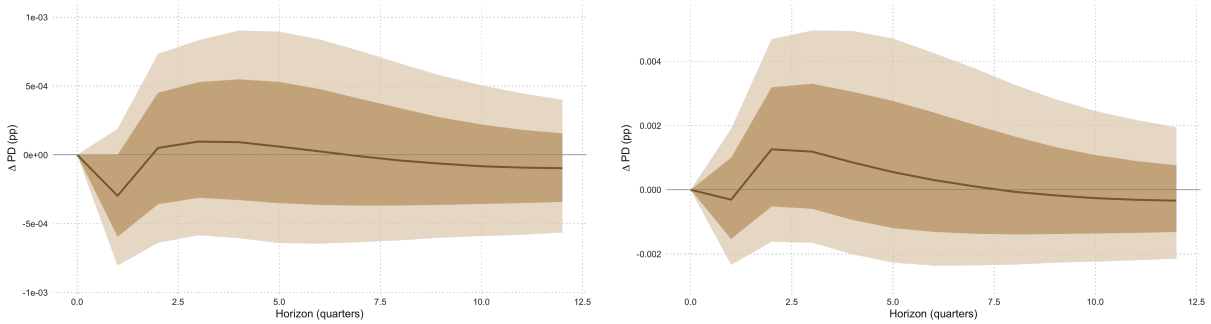

(a) PD — one-sd shock

(b) PD — 09/11 shock

Figure 10: Comparison of Probabilities of Default under a one-sd schock and a calibrated GPR Shock (2001Q3/9-11) (PD)

Notes: Panel (a) presents the generalized impulse response function (IRF) for a one-standard-deviation shock to GPR on the PD, derived from both the VAR and the satellite models. Panel (b) presents the IRF for a calibrated GPR shock (2001Q3/9-11) on the PD, also derived from the VAR and the satellite models. The posterior medians are shown as solid lines, with 68% (dark) and 90% (light) pointwise credible intervals indicated.

Both panels display hump–shaped responses with a one–quarter delay. In Figure 10a, a one–standard–deviation geopolitical shock induces a small dip at $h \approx 1$, followed by a modest peak at $h = 2$–3 that gradually reverts toward zero by $h \approx 7$; the predictive distribution remains centered close to zero, with wide credibility bands indicating substantial uncertainty around the median response. By contrast, Figure 10b (9/11 scenario) exhibits the same timing but a markedly larger and more persistent rise—roughly three to four times the baseline amplitude. Although the outer credibility bands still include zero, the posterior distribution assigns a higher probability to a positive effect over horizons $h \approx 2$–6, suggesting that the increase in PD is more

likely under this scenario.

A.8 Alternative Application: Delinquency Rate as a Default-Risk Proxy

In this section, we replicate the empirical application used in the main part of the paper. As an alternative proxy for U.S. banks' default risk, we use the *Delinquency Rate on All Loans, All Commercial Banks (DRALACBN)*[8]. The delinquency rate is the share of outstanding loans that are past due beyond a specified threshold (typically 30+ days) and/or placed on nonaccrual status; it is a portfolio-level measure of payment arrears rather than a formal default event. By contrast, under the Basel IRB framework, a default is recognized at the obligor level when the bank judges the obligor unlikely to pay its credit obligations in full without recourse to collateral, or when any credit obligation is more than 90 days past due (180 days for certain retail/public-sector exposures). Once default is triggered, all of the obligor's exposures are considered in default. Thus, while delinquency tracks overdue payments on individual loans, IRB default captures a broader credit event used for PD/LGD/EAD calibration; the two notions are related but not interchangeable.

Relative to the EBA dataset used in the main analysis, the DRALACBN series is longer and more readily available, yielding 162 quarterly observations (versus 37 for the EBA). We therefore rely on DRALACBN in this section (see Figure 11).

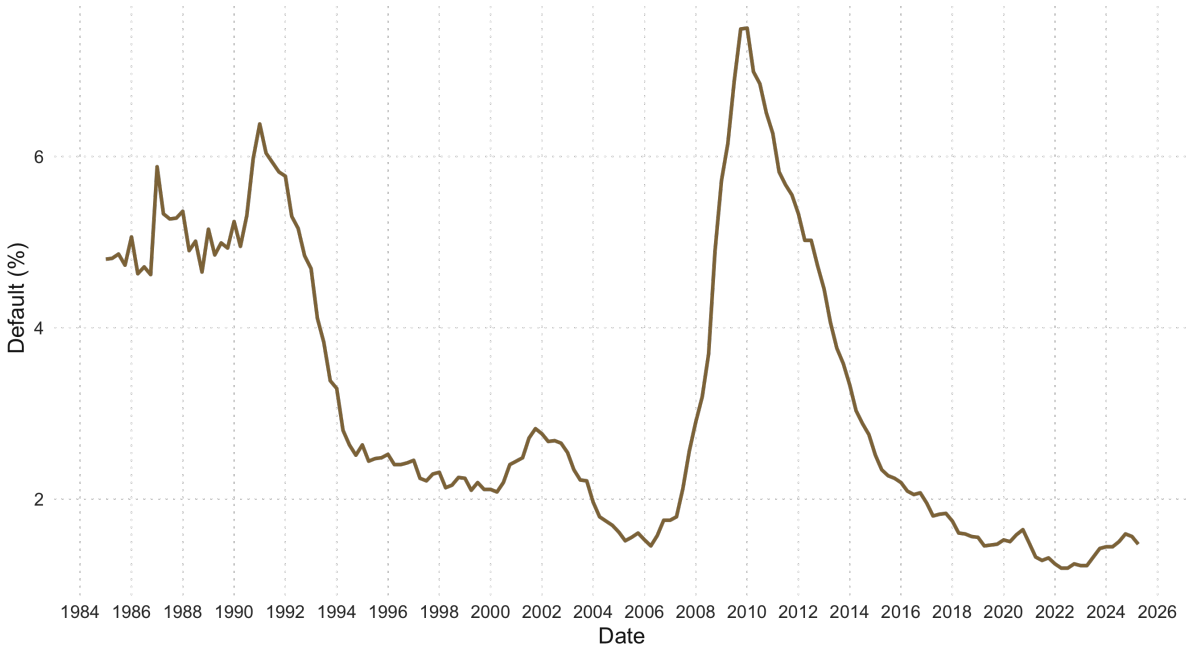

Figure 11: Delinquency rate on all loans at U.S. commercial banks (DRALACBN). *Quarterly series; percent of loans 30+ days past due and/or on nonaccrual. Source: Federal Reserve Bank of St. Louis (FRED).*

[8] https://fred.stlouisfed.org/series/DRALACBN

To characterize the economy's dynamics, we first fix the VAR environment. We adopt the S5 specification (Table 3) as our baseline. His specification is stable, with 62% of posterior draws inside the unit circle, and produces smooth, economically interpretable impulse responses. It ensures meaningful shock identification, avoiding over-parameterization. The chosen ordering for quarterly data is as follows: (i) geopolitical risk is exogenous; (ii) investment reacts quickly to uncertainty; (iii) hours adjust after output due to labor frictions; (iv) the real oil price responds to demand conditions with a delay; (v) inflation is placed last to respond to all shocks. The impulse response functions (IRFs) for a one-standard deviation increase in geopolitical risk are shown in Figures 9.

Table 9: Out-of-sample best model

Dependent variable: Z		
	Estimate	**Std. Error**
Intercept	0.0371	0.0303
log_inv_pc_lag1	0.0345***	0.00154
log_hours_pc_lag0	0.0293**	0.0110
log_oil_real_lag1	-0.0082***	0.00136
log_oil_real_lag4	-0.0028*	0.00134
infl_yoy_pct_lag1	0.1027***	0.0225
Out-of-sample performance (test set)		
RMSE		0.4494
MAE		0.3267
R^2_{OOS}		0.8450
In-sample fit (training sample)		
Residual std. error	0.375	(df = 148)
R^2 / Adj. R^2	0.8632 /	0.8585
Observations		154

Model specification (selection stage). Lag order $p = 4$; at most 6 predictors per candidate model.
Selection criterion. Models ranked by out-of-sample RMSE (tie-breaker AIC).
Estimation. OLS with conventional standard errors. Standard errors shown in the second column.
Significance. * $p < 0.05$, ** $p < 0.01$, *** $p < 0.001$.

The second step involves estimating the systematic factor Z. Given the increased number of data points, we select the model that performs best out-of-sample (OOS). Table 9 presents the results, where all selected predictors are precisely estimated and economically meaningful. The lagged investment per capita and hours worked per capita variables both have positive effects on Z, suggesting a procyclical relationship. Specifically, a 1% increase in investment per capita one quarter ago and hours worked per capita today are associated with an increase in Z of approximately 0.034 and 0.029, respectively. On the other hand, the lagged real oil

price and inflation rate show negative effects, with a 1% increase in real oil prices one and four quarters ago leading to a decline in Z by about 0.008 and 0.003, respectively. The out-of-sample performance is strong ($R^2_{\text{OOS}} = 0.845$, RMSE $= 0.449$), significantly outperforming in-sample metrics ($R^2 = 0.8632$, residual standard error $= 0.375$), and suggests minimal overfitting given the model's parsimonious nature.

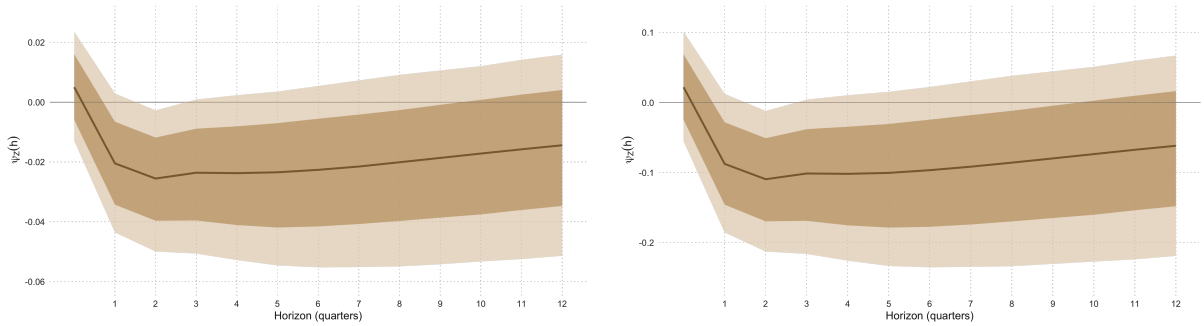

(a) Z — one-sd shock **(b)** Z — 09/11 shock

Figure 12: Comparison of systemic factor Z under a one-sd schock and a calibrated GPR Shock (2001Q3/9-11)

Notes: Panel (a) presents the generalized impulse response function (IRF) for a one-standard-deviation shock to GPR on Z, derived from both the VAR and the satellite models. Panel (b) presents the IRF for a calibrated GPR shock (2001Q3/9-11) Z, also derived from the VAR and the satellite models. The posterior medians are shown as solid lines, with 68% (dark) and 90% (light) pointwise credible intervals indicated.

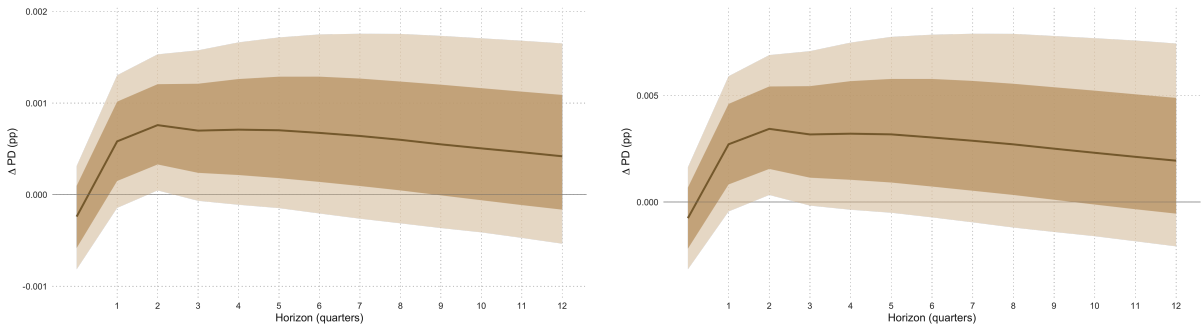

(a) PD — one-sd shock **(b)** PD — 09/11 shock

Figure 13: Comparison of Probabilities of Default under a one-sd schock and a calibrated GPR Shock (2001Q3/9-11) (PD)

Notes: Panel (a) presents the generalized impulse response function (IRF) for a one-standard-deviation shock to GPR on the PD, derived from both the VAR and the satellite models. Panel (b) presents the IRF for a calibrated GPR shock (2001Q3/9-11) on the PD, also derived from the VAR and the satellite models. The posterior medians are shown as solid lines, with 68% (dark) and 90% (light) pointwise credible intervals indicated.

Figures 12 and 13 compare the probability of default (PD) under two disturbances: a one-standard-deviation geopolitical shock (right panels) and the 9/11 scenario (left panels). Consistent with the empirical results in Section 4.2, the geopolitical shock raises the PD starting at horizon $h = 1$ and then gradually reverts toward zero after $h = 3$.

A.9 Macro–financial variables: definitions and transformations

Table 10: Macro–financial variables, definitions and transforms

Code	Definition	Transform / Unit
Baseline VAR		
`log_GPRD`	Log geopolitical risk index (Caldara and Iacoviello (2022)).	log level; quarterly avg.
`vix`	CBOE Volatility Index (FRED: `VIXCLS`).	Level; quarterly avg (index).
`log_sp500_real`	Real S&P 500 (Adj Close deflated by CPI).	log real level.
`log_oil_real`	Real WTI spot (FRED: `WTISPLC`) deflated by CPI.	log real level.
`log_hours_pc`	Nonfarm business hours per capita (HOANBS / CNP16OV).	log; per capita.
`log_gdp_pc`	Real GDP per capita (GDPC1 / CNP16OV).	log; per capita.
`nfci`	National Financial Conditions Index (Chicago Fed).	Level (index; > 0 tighter).
Robustness variables		
`gs2`	U.S. Treasury 2Y yield (constant maturity).	Level; quarterly avg (%).
`t10Y2Y`	10Y minus 2Y Treasury spread.	Level (pp).
`t10Y3M`	10Y minus 3M Treasury spread.	Level (pp).
`infl_yoy_pct`	CPI year-over-year inflation.	$100[\log(\text{CPI}_t) - \log(\text{CPI}_{t-4})]$.
`infl_annualized_pct`	CPI quarter-on-quarter, annualized.	$400[\log(\text{CPI}_t) - \log(\text{CPI}_{t-1})]$.
`gdp_yoy_pct`	Real GDP year-over-year growth.	$100[\log(\text{GDP}_t) - \log(\text{GDP}_{t-4})]$.
`log_inv_pc`	Real private investment per capita.	log; per capita.
`epu`	Economic Policy Uncertainty index (Baker et al. (2016)).	Level; quarterly avg (index).

Notes: "Real" variables deflated by CPI (`CPIAUCSL`); per-capita divides by civilian population 16+ (`CNP16OV`). Higher-frequency series are averaged to calendar quarters. "pp" = percentage points.